NAVAL POSTGRADUATE SCHOOL

MONTEREY, CALIFORNIA

THESIS

FLUID-FILLED STRUCTURE WITH MULTIPLE COMPOSITE COMPARTMENTS SUBJECTED TO LOW-VELOCITY IMPACT

by

Joshua D. Bowling

June 2018

Thesis Advisor: Young W. Kwon
Second Reader: Jarema M. Didoszak

THIS PAGE INTENTIONALLY LEFT BLANK

REPORT DOCUMENTATION PAGE	*Form Approved OMB No. 0704-0188*

1. AGENCY USE ONLY *(Leave blank)*	**2. REPORT DATE** June 2018	**3. REPORT TYPE AND DATES COVERED** Master's thesis

4. TITLE AND SUBTITLE FLUID-FILLED STRUCTURE WITH MULTIPLE COMPOSITE COMPARTMENTS SUBJECTED TO LOW-VELOCITY IMPACT	**5. FUNDING NUMBERS**
6. AUTHOR(S) Joshua D. Bowling	
7. PERFORMING ORGANIZATION NAME(S) AND ADDRESS(ES) Naval Postgraduate School Monterey, CA 93943-5000	**8. PERFORMING ORGANIZATION REPORT NUMBER**
9. SPONSORING / MONITORING AGENCY NAME(S) AND ADDRESS(ES) N/A	**10. SPONSORING / MONITORING AGENCY REPORT NUMBER**

11. SUPPLEMENTARY NOTES The views expressed in this thesis are those of the author and do not reflect the official policy or position of the Department of Defense or the U.S. Government.

12a. DISTRIBUTION / AVAILABILITY STATEMENT Approved for public release. Distribution is unlimited.	**12b. DISTRIBUTION CODE** A

13. ABSTRACT (maximum 200 words)

The focus of this study was to investigate the dynamic response and the fluid-structure interaction (FSI) in a fluid-filled composite structure with multiple compartments subjected to a low-velocity impact. The compartments were used to simulate multiple structures separated by a fluid medium. The design apparatus was fabricated from Polymethly Methacrylate (PMMA) plastic components and carbon fiber sheets with varying thicknesses. The structure was struck with a low-velocity impact from a spherical object attached to a pendulum and the oscillatory motion of the fluid within the container was analyzed. The design structure was filled at multiple water levels to study the impact of the added mass and fluid coupling effects that are attributed to the amount of water in the structure and the distance between the plates.

The measurable quantities are the impact force, the strain gauges attached to the carbon fiber sheets and the natural frequency of the fluid within the structure. The results showed that the FSI and the dynamic response was significantly increased due to the rise in water fill level and that the resonance frequency of the structure decreased with an increase in water level. The distance between structures was also significant but not as predictable as the fill level and must be monitored closely in future designs using experimental testing during the design process.

14. SUBJECT TERMS fluid-structure interaction composite, structural coupling through fluid	**15. NUMBER OF PAGES** 85
	16. PRICE CODE

17. SECURITY CLASSIFICATION OF REPORT	**18. SECURITY CLASSIFICATION OF THIS PAGE**	**19. SECURITY CLASSIFICATION OF ABSTRACT**	**20. LIMITATION OF ABSTRACT**
Unclassified	Unclassified	Unclassified	UU

NSN 7540-01-280-5500 Standard Form 298 (Rev. 2-89) Prescribed by ANSI Std. 239-18

THIS PAGE INTENTIONALLY LEFT BLANK

Approved for public release. Distribution is unlimited.

FLUID-FILLED STRUCTURE WITH MULTIPLE COMPOSITE COMPARTMENTS SUBJECTED TO LOW-VELOCITY IMPACT

Joshua D. Bowling
Lieutenant, United States Navy
BSE, University of South Carolina, 2011

Submitted in partial fulfillment of the
requirements for the degree of

MASTER OF SCIENCE IN MECHANICAL ENGINEERING

from the

NAVAL POSTGRADUATE SCHOOL
June 2018

Approved by: Young W. Kwon
Advisor

Jarema M. Didoszak
Second Reader

Garth V. Hobson
Chair, Department of Mechanical and Aerospace Engineering

THIS PAGE INTENTIONALLY LEFT BLANK

ABSTRACT

The focus of this study was to investigate the dynamic response and the fluid-structure interaction (FSI) in a fluid-filled composite structure with multiple compartments subjected to a low-velocity impact. The compartments were used to simulate multiple structures separated by a fluid medium. The design apparatus was fabricated from Polymethly Methacrylate (PMMA) plastic components and carbon fiber sheets with varying thicknesses. The structure was struck with a low-velocity impact from a spherical object attached to a pendulum and the oscillatory motion of the fluid within the container was analyzed. The design structure was filled at multiple water levels to study the impact of the added mass and fluid coupling effects that are attributed to the amount of water in the structure and the distance between the plates.

The measurable quantities are the impact force, the strain gauges attached to the carbon fiber sheets and the natural frequency of the fluid within the structure. The results showed that the FSI and the dynamic response was significantly increased due to the rise in water fill level and that the resonance frequency of the structure decreased with an increase in water level. The distance between structures was also significant but not as predictable as the fill level and must be monitored closely in future designs using experimental testing during the design process.

THIS PAGE INTENTIONALLY LEFT BLANK

TABLE OF CONTENTS

LIST OF FIGURES

THIS PAGE INTENTIONALLY LEFT BLANK

LIST OF TABLES

THIS PAGE INTENTIONALLY LEFT BLANK

LIST OF ACRONYMS AND ABBREVIATIONS

FSI	Fluid Structure Interaction
CFRP	Carbon Fiber Reinforced Polymer
HRAM	Hydrodynamic Ram
NPS	Naval Postgraduate School
PMMA	Polymethyl Methacrylate
CAD	Computer-Aided Design

THIS PAGE INTENTIONALLY LEFT BLANK

ACKNOWLEDGMENTS

I would like to take the time to express my appreciation for the dedication of my thesis advisor, Professor Young Kwon. You introduced the material and engaged my interest in the field of solid mechanics and fluid-structure interactions (FSI). Thank you for the guidance, mentorship and patience while I conducted my research and explored the vast topic of fluid coupling. I would also like to thank Professor Jarema Didoszak, Mr. John Mobley and Dr. Chanman Park for their support and guidance during the testing phase of my project.

Most importantly, I would like to thank my family for their unwavering support of my graduate studies. To my daughter, Grace, I love the passion you have for science and engineering. I am so happy that you were able to help me conduct my lab tests and data analysis. I hope you continue to grow and thrive in the fields of mathematics and engineering. To my beautiful wife, Regina, thank you for being my rock and keeping our family afloat while I studied. Your unwavering dedication to the success of our little family is an inspiration for my work.

THIS PAGE INTENTIONALLY LEFT BLANK

I. INTRODUCTION

A. BACKGROUND

Fluid Structure Interaction (FSI) is a phenomenon that occurs naturally in many engineering problems due to the large number of structures that are in contact with fluids. Disciplines such as hydrodynamics, mechanics, civil and biomedical deal with problems that must examine an FSI solution. Structures designed to hold a fluid, such as ballast tanks, water pipes and blood vessels, must take into account the change in system inertia due to the added mass of the fluid. These systems, coupled with impacts that can cause sloshing effects, can have a great impact on the internal stability of the structure. Composite materials are becoming more common and replacing metals in these systems due to their low weight, high strength and performance characteristics. Composite materials are lighter than their predecessors and in turn have a greater FSI. Due to composites having similar densities to water, the FSI between the two; plays a very significant role in design [1]. The dynamic response of the material is an essential parameter to consider in order to avoid system failure.

1. FSI Single Compartment Structure

The added mass of the fluid within a structure adds stress to the structure when the fluid is excited by an external force. Experimental results show that the stress propagation from the front side to the back side of a solid structure when the front side is struck with an object at a low-velocity, is significant, depending on the amount of water inside the structure [2]. Defense applications for composites remain minimal due to the material's reduced hardness and ductility. Aslan et al. [3] states that "If a composite laminate is subjected to a low-velocity impact of sufficient energy, it may create damage consisting of internal delamination of the composite." Delamination would cause the structure to begin to leak and ultimately fail. The composites used in prior FSI research are composed of carbon fiber reinforced polymer (CFRP) composites and E-glass woven with resin composites [2]–[6], all of which found that FSI had a substantial effect on the dynamic response of the structure [2]. Previous research also focused on the stress profiles within a

solid structure [2]–[6]. This research measured the stress of two independent structures, coupled together by a fluid medium.

Similar studies focus on high-velocity impacts and the hydrodynamic ram (HRAM) effect at multiple fill levels. HRAM is the study of a high-velocity projectile influencing a structure filled with a fluid and the damage that occurs due to the added mass of the fluid. Varas et al. used rectangular structures and measured the pressure, strain and the associated deformation that occurred within the structure due to the HRAM and FSI phenomena. Their studies found that the fluid has a significant effect on the structure's deformation and eventual failure [7]–[9].

2. FSI Coupled Structure

The flexibility of composite material is of great interest when using structures coupled by a fluid medium. The energy from the impact face of one structure will be transferred to another structure due to the coupling effects of the structures and the fluid medium between them [10]. Composites used for defense applications are required to be robust in order to withstand uncertainties found in a dynamic environment. This research used engineered carbon fiber composite sheets that are comprised of orthotropic laminates using a twill weave at 0/90-degree orientation [11]. This research also discussed the experimental results of the FSI effects on a structure that is filled with a fluid medium at multiple fill levels and the dynamic response of multiple structures when coupled with the fluid. Many numerical studies conducted on fluid filled structures, metals and composites, study the sloshing effect to determine the modal mass and stiffness matrices of the fluid filled tanks, as well as the critical structural frequencies. However, these studies do not discuss the failure criteria due to low-velocity impacts on coupled structures [12]–[14]. Numerical studies have been conducted to measure the frequency of the tank motion and determine if it is close to the natural frequency of the fluid medium [15]. The structural coupling through a fluid medium has been examined numerically but has not been completed experimentally for comparison.

B. OBJECTIVE

The objective of this research was to analyze the FSI effect on a composite structure with multiple compartments, filled with a fluid and subjected to a low-velocity impact. The experiment is used to simulate the structural coupling between two structures separated by a fluid medium. The independent variables that are altered during the tests were the water fill levels and the distance between the two structures. The coupling effect between the two structures is the primary focus of this research and used to determine if the maximum stress on the second structure can be attributed to the distance between the structures and the height of the water between them. Two separate structures were used for data analysis. The first structure was the basis for a previous Naval Postgraduate School (NPS) thesis topic [2] and was tested to validate the bifurcation effect that the student noticed in the data analysis. This experiment is labeled as Design I and the testing is labeled Phase 1 and Phase II for simplicity.

The second apparatus analyzed was the basis for this research and labeled as Design II. Design II has multiple compartments used to simulate two structures separated by a fluid medium. The tests consisted of monitoring the dynamic response on the structures as the force of an impact device is transferred between the structures. Understanding how the structure responds to the dynamic behavior of the coupled compartments will assist engineers in future composite designs. The coupling effect between the two structures caused the second structure to vibrate when the impact force struck the first structure. The maximum amount of stress, strain and deformation is of particular interest for future designs where the medium between the compartments, fill level and distance between structures may vary due to design.

THIS PAGE INTENTIONALLY LEFT BLANK

II. EXPERIMENTAL PROCEDURE

A. DESIGN STRUCTURE FABRICATION

Prior research conducted at NPS pertaining to FSI involved low-velocity impacts on carbon fiber rigid boxes [10], [3]. The stress on the designs was increased due to the added mass effect of water. Higher fill levels inside the structure allowed a larger force to penetrate the structure and caused greater amounts of stress as the water propagated through the structure. The previous research involved one structure with a single compartment. This study focused on a structure with multiple compartments that can be altered to give the structure different compartment sizes. The compartments are designed to simulate independent structures that are separated by a fluid medium. When struck with a low-velocity impact device, the fluid caused a coupling effect between the structures that was studied along with the added mass of the fluid. The multiple compartments allowed the volume of fluid to change and the proximity between the structures to vary so the coupling effects could be further analyzed.

1. Design Criteria

The test structure met a variety of design characteristics. The design had multiple compartments in order to study the effects of fluid coupling. Fluid coupling was magnified by the distance between structures so the structure had compartments that were altered without creating multiple apparatuses. The structure was water tight to account for the change in water level between experiments, as to study the added mass effect due of the FSI. Previous design structures were fabricated under vacuum using E-glass fiber sheets and resin [1], [3] and [10]. A structure with multiple compartments would be difficult to fabricate using the vacuum seal method, so it was simulated using multiple types of material. In order to meet the multiple compartment design criteria, the apparatus was constructed out of Polymethly Methacrylate (PMMA), aluminum and carbon fiber sheets. The carbon fiber sheets was used to simulate the composite structures that are coupled by the fluid as well as the impact and test surfaces. The PMMA material was used as the walls and top of the structure and provided rigidity to constrict movement of the composite

sheets. The PMMA sheets also allowed the motion of the fluid to be observed during the experiment. The bottom plate of the structure is a solid aluminum base, which is lightweight and used to restrict the movement of the system. The entire setup was secured to a vibration isolation table to limit the external vibrations felt during testing.

The criteria that was met in the design process included restricting the movement of the carbon fiber sheets to zero degrees of freedom. The sections were also water tight to avoid liquid leaking between the compartments. The watertight compartments could also be used to separate multiple liquids at different densities for future tests. The final attribute to the design allowed the structure to house carbon fiber sheets of varying thicknesses. Allowing sheets of different thickness levels will give the design engineer options to change many independent variables in the design. The thickness of the structure can be changed, the number of compartments can vary, multiple fluids can be tested simultaneously and the impact force can be increased and successfully replicated.

2. Material Selection and Properties

Dragon Plate Inc. manufactured the composite plates used in this experiment. The company specializes in orthotropic and quasi-isotropic laminates using a carbon reinforced epoxy matrix without core material [11]. The quasi-isotropic material is more robust due to the lay-up manufacturing process of 90-degree and 45-degree fabric sheets. The impact forces used in this experiment will be minimal, therefore, the orthotropic, economy plate, was chosen for this design.

The material properties of the orthotropic sheets are of significant importance. The density of the material was measured to be 1380 kg/m^3. The modulus of elasticity was measured using an Instron 4507 tensile testing machine. Tensile test samples were taken from multiple sheets and cut at 0, 45 and 90-degree orientations. The cuts, labeled A for 0 degrees, B for 90 degrees and C for 45 degrees, can be seen in Figure 1.

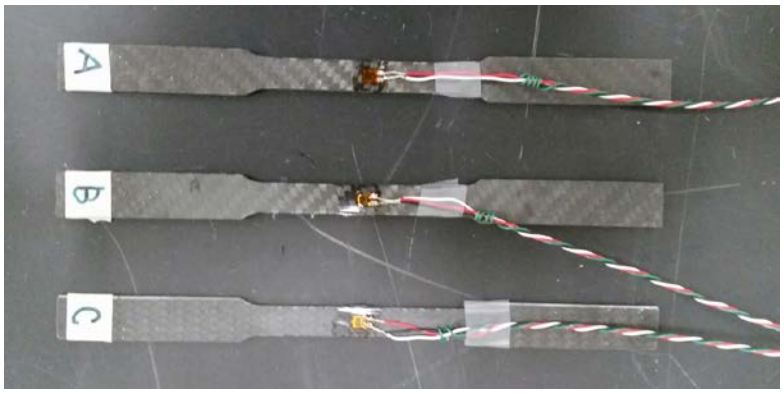

Figure 1. Tensile Test Samples of Carbon Fiber Sheets

The strength of the material gave an estimate for the amount of impact force that can be applied to the structure once it is filled to 100%. If the integrity of the structure is compromised, the fluid will leak and damage the measurement equipment. The material being tested is shown in Figure 2 and the results of failure can be seen in Figure 3.

Figure 2. Instron 4507 Tensile Testing Machine

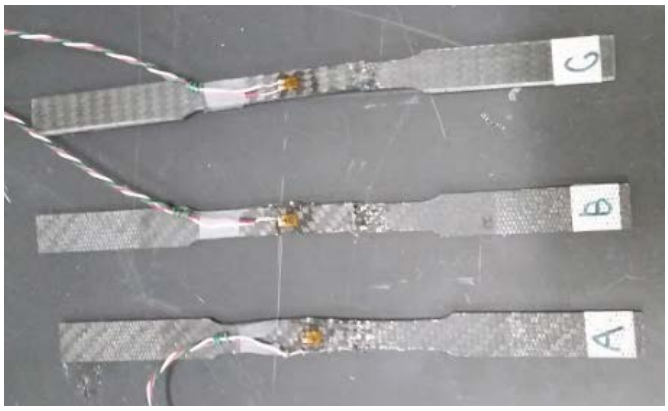

Figure 3. Location of Failure for all Three Tensile Test Samples

The failure point for all three samples was directly above the strain gauge within the test area. The material maintained a very consistent modulus for the 0-degree and 90-degree samples and the modulus for sample C was very small due to the layup of the composite sheets as shown in Table 1.

Table 1. Material Properties of Dragon Plate Composite Economy Sheets

Tensile Test Results		
Test Sample	**Max Load (kN)**	**Youngs Modulus (GPa)**
A (0 Degrees)	33.6	58.95
B (90 Degrees)	25.8	54.48
C (45 Degrees)	34.6	15.83

3. Fabrication

The model was designed to secure the carbon fiber sheets to restrict their freedom of movement. Creo Parametric 3.0 was the modeling software used in the design. The PMMA side panels are the white panels in Figure 4 and the machined parts are shown in Figure 5. The side panels fit snuggly inside 12.7mm thick notches in the aluminum base as shown in Figure 6. The PMMA sheets were secured to the aluminum base using silicone and RTV sealant. Both the side panels and the aluminum base have notches cut out at every 3.175mm so the carbon fiber sheets can slide inside of them. The Computer-Aided Design (CAD) drawings of the structural components are in the Appendix.

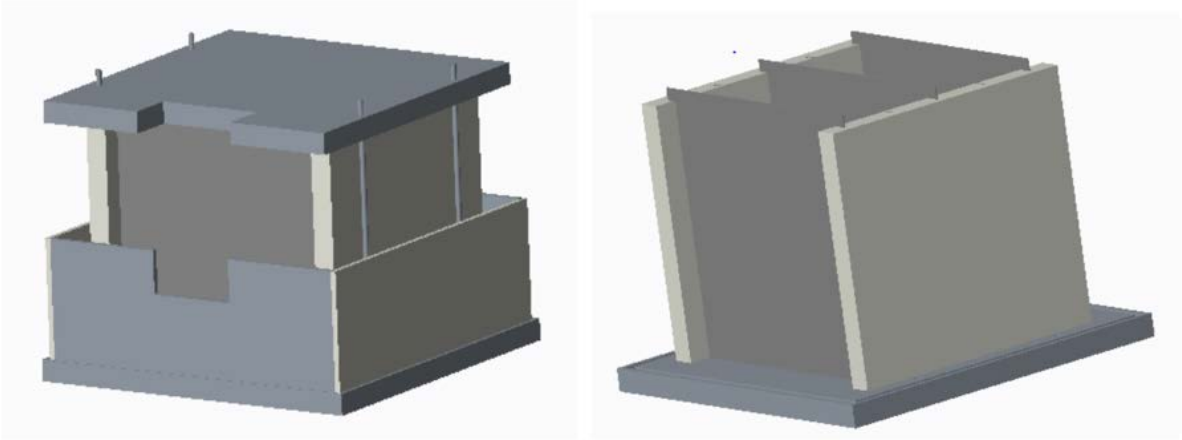

Figure 4. Creo Parametric 3.0 Model of Structure

Figure 5. Isometric View of Side Panel

The model has five notches cut out to house four fluid filled sections. The sections correspond to the grooves cut into the material with Section I being the smallest section and Section IV having the greatest fluid volume. The base plate also has four holes threaded at 6.35mm-28 to secure the top plate with four 356mm bolts as shown in the model in Figure 6. The final attribute of the base plate is the 12.7mm groove cut around the edge of the plate. The groove houses a 152.5mm external barrier that will catch leaking water in the instance the carbon fiber sheets fail, either due to impact or due to loading.

Figure 6. Bottom Plate with Slots and Securing Holes

The top plate is also constructed out of PMMA and has the same notches as the sides and base plate as seen in Figure 7. The three test sections are labeled in Figure 7 with the distance measurements between each plate listed. The four holes in the top plate line up with the holes in the base plate so four bolts can slide through the top plate and restrict movement of the structure. The square notch cut in the top plate is used to allow the swinging impact pendulum room to strike the front face of the carbon fiber sheets without damaging the top plate. The complete setup at fill Section IV can be seen in Figure 8 with the top plate removed.

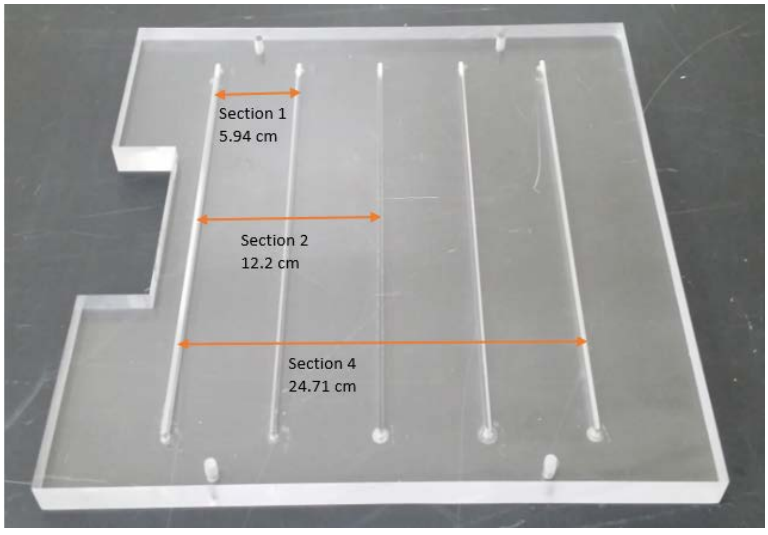

Figure 7. Top Plate with Slots

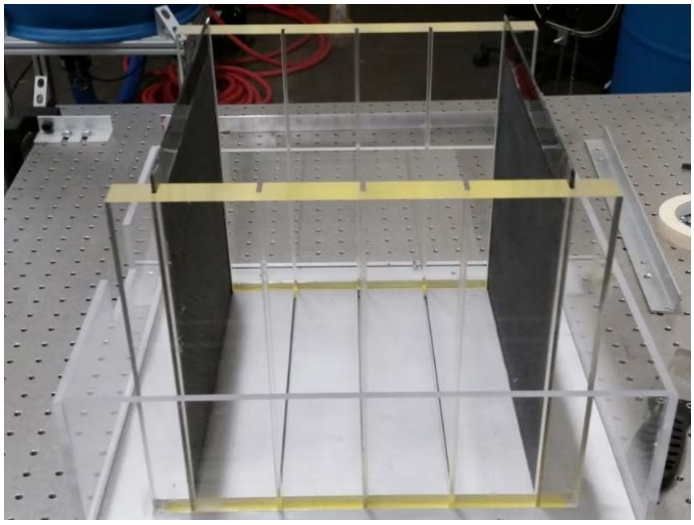

Figure 8. Design Structure at Section IV Setup

The slots in the material are cut to 3.175mm to allow analysis of composite sheets at various thickness. The sheets used for the initial tests are 1.60mm. The gap between the sheet and the PMMA sides and aluminum base was filled with a composite strip of equal thickness measured at 305mm x 12.7mm. Three of these strips held the composite sheet into place while the top edge had a Plexiglas sheet of equal thickness adhered as shown in Figure 9.

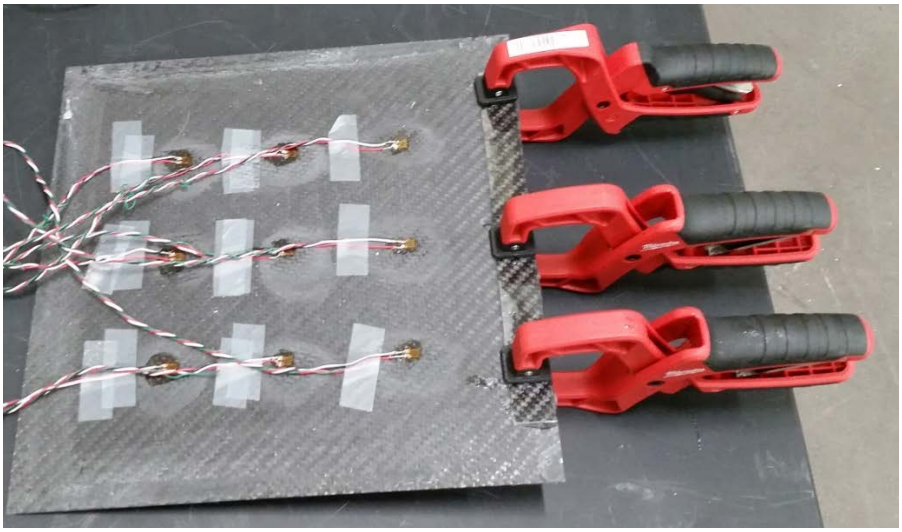

Figure 9. Adhesion of Plexiglas Strip to Composite Sheet

Clear silicone was placed on all of the gaps of the structure prior to assembly to create a watertight barrier. Once the sheets were in place, the silicone was applied around the inner and outer edges of the sheets. The silicone was allowed to dry for 24 hours prior to conducting experiments. A leak test was also conducted prior to experimental testing to demonstrate the structural integrity of the system.

B. TEST EQUIPMENT INSTALLATION

1. Experiment Setup

The experimental setup consisted of the structure at the designed section fill level, eighteen strain gauges, a swinging pendulum used as the impact device and a load cell connecting the pendulum to the LabView data acquisition software. The impact device's setup was not altered from Design I to Design II. The construction and operation of the impact device created a repeatable low-velocity impact [2]. The pendulum was released from a 45-degree angle for each test. The angle was measured using a fixed protractor so that the tests would be repeatable.

2. Strain Gauge Placement

Nine strain gauges were installed on the carbon fiber sheets to measure the strain in the y-direction only. Previous studies proved that the strain remained consistent between the x-direction and y-direction, so only one direction was used for this research [1], [10]. The gauges were manufactured by MicroMeasurements and had a grid resistance of 350 ohms and nominal gauge factor of 2.15. The part number for the gauges is CEA-13–125WT-350. The strain gauges were installed evenly spaced apart from one another in the center of each carbon fiber sheet.

a. Surface Preparation

The surface was prepared using fine-grit sand paper to smooth the surface. It was then cleaned using a gauze soaked with ethanol and finally cleaned with a gauze soaked with methanol. The gauges were placed on the measured marks using cellophane tape to keep the gauges in place during curing.

b. Gauge Adhesion

The gauges were placed on the sheet and a piece of cellophane tape was used to keep the gauge in place during the 24-hour curing phase. A MicroMeasurements M-Bond AE-10 Adhesive kit containing a two-part epoxy was used to bond the strain gauges to the sheet. The kit contained resin and was mixed with 10mL of hardener for 15 minutes prior to being applied to the gauges. Figure 10 shows the gauge placement for Phase I and Phase II testing of Design I.

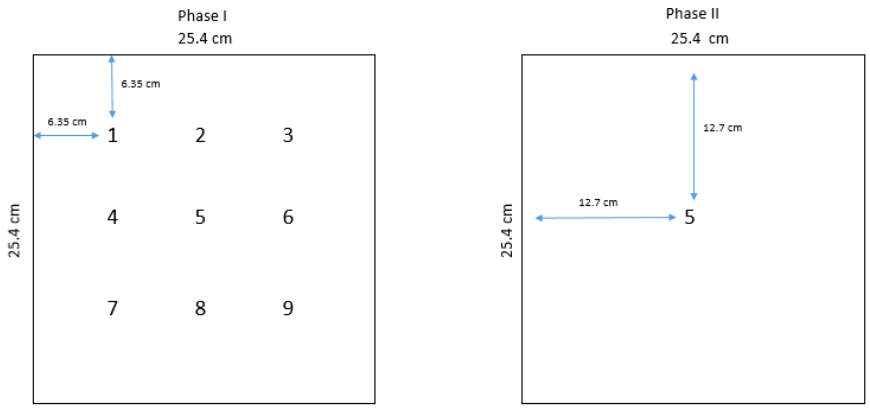

Figure 10. Design I Gauge Placement

Figure 11 shows the gauge placement for the front face and back face of Design II. The center gauge for the front face was offset as not to impede the impact device. The center gauge on the front face was offset to allow the impact device to strike the center of the plate.

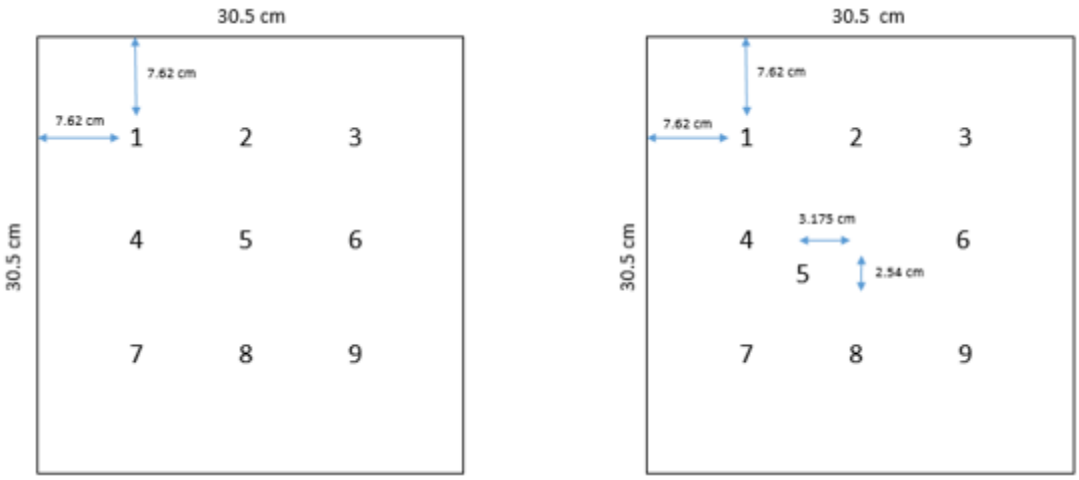

Figure 11. Design II Gauge Placement

c. Wire Placement and Testing

The lead wires were soldered to the pads on the strain gauges in accordance with Figure 12. The wire leads were tested with a micrometer to ensure they were not damaged during installation and read 350 ohms.

Figure 12. Wire Lead Placement

3. Data Acquisition Setup

The measurable data for this experiment was the impact force and the strain readings from the gauges. The data was collected using the NI LabVIEW Signal Express 2012 software suite. The full list of components and LabVIEW settings are described in detail in the Appendix. The data was extracted from LabVIEW as .txt files and analyzed using MATLAB.

C. METHODOLOGY

The experimental set-up was designed to study the coupling between the two carbon fiber sheets. The sheets acted independently due to the manner in which they were fixed in the apparatus to simulate two structures. The low-velocity impact device initiated the fluid coupling due to the FSI between the structure and the fluid. To properly study the effects of fluid coupling and the FSI, the structure was tested under multiple conditions to attain an appropriate sample size. The focus of this research was to continue studying the FSI effects on a structure filled with water and the impact of the force over multiple compartments. Design I underwent two phases of testing to test the stress on the front and back face of the structure. Both phases were studied to validate the bifurcation experienced in previous research. Design II was then constructed and tested to study the fluid coupling effects caused by the FSI on multiple structures.

1. Design I Testing

Design I testing was conducted in two phases and consisted of re-creating tests that were previously completed by South and Pentaleri [2], [16]. South noted that a bifurcation existed in the maximum strain on the back face of the structure. Only the back face of Design I was analyzed during this testing since it is the location of the bifurcation observed in previous tests. The gauges on the front and sides were studied in previous research and their locations are shown in Figure 13.

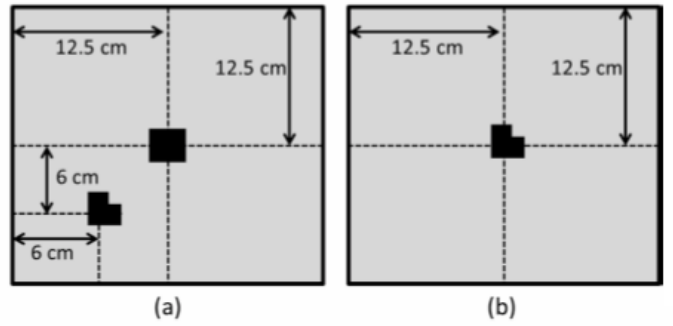

Figure 13. Strain Gauge Locations on (a) the Front Side and (b) the Left, Right and Back. Source: [2].

South [2] showed that a bifurcation existed in the strain frequencies on the center gauge on the structure's back face. Exactly half of the tests showed max strain in compression while the other half of the tests were in tension, as shown in Figure 14. This data led South to conclude that a bifurcation existed on the back face of the structure and recommended that future studies work to further investigate this phenomenon.

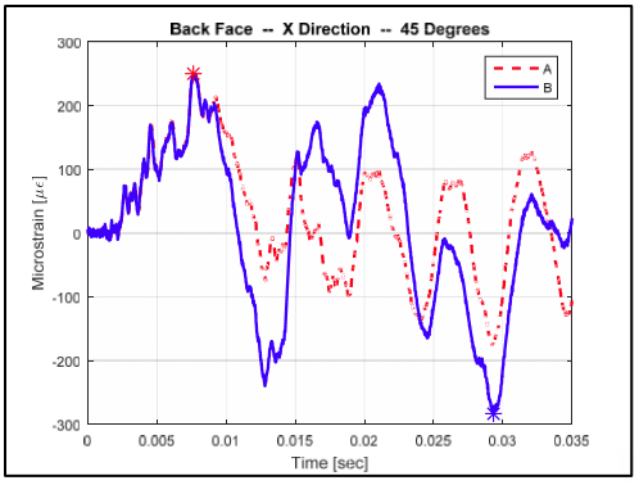

Figure 14. Strain Bifurcation at 50% Fill Level. Source: [2].

The research completed by Pentaleri was used to validate South's research by placing eight extra gauges on the box to get a full strain field as shown in Figure 15. The tests were conducted when the box was filled to 50% to recreate the bifurcation. Multiple tests were run on the box and showed some gauges in tension while others were in compression but failed to reproduce the bifurcation at any specific location [16].

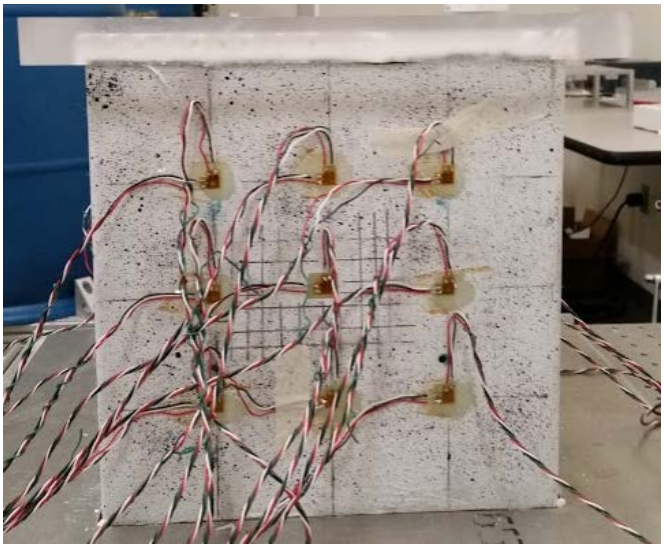

Figure 15. Strain Tests: Nine Biaxial Gauges

Phase I of this research was to repeat the tests completed by Pentaleri and compare them to his results. Phase II of testing was to remove the additional eight gauges added by Pentaleri and replicate the original tests conducted by South as shown in Figure 16. Both phases of testing were compared with South and Pentaleri's data to verify whether or not a bifurcation could be replicated on the back face of the solid structure.

Ten tests were conducted on the box during Phase I with all nine gauges attached and ten tests were conducted for Phase II with only the center gauge left intact to measure the effects of the FSI. The tests were conducted at the 0%, 25%, 50%, 75% and 100% fill levels. The only change made to the structure between all three researchers was the addition of eight gauges to the back face and then removing the additional eight gauges at the end. In theory, altering the gauge placement on the box should not alter the results measured by the center gauge. The results from Phase II matched the results of Phase I. The bifurcation

phenomena was not replicated but was further examined while conducting tests on Design II.

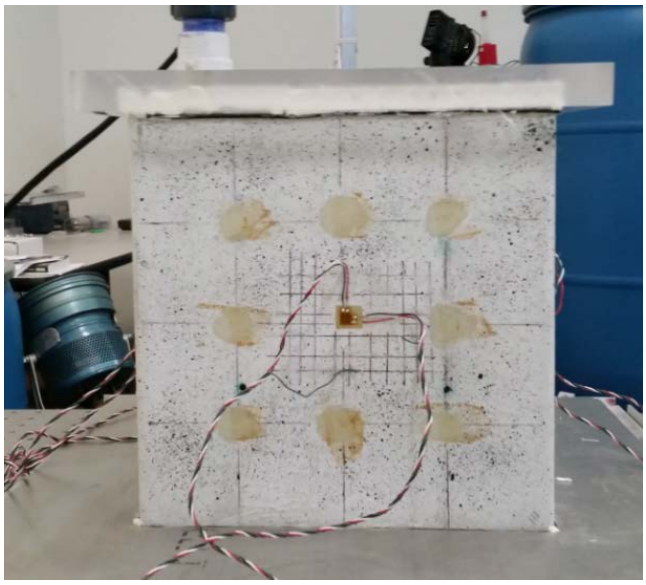

Figure 16. Strain Tests: Center Strain Gauge Only

2. Design II Testing

Design II testing used the structure fabricated to study the coupling effect caused by the FSI. Only Sections I, II and IV were tested. Section III was not tested because it was deemed redundant to determine the behavior of the FSI between the water and the plates. The first set of testing was conducted at fill Section II on the 1.60mm sheets. Nine strain gauges were placed on both the front and back sheets to determine the full strain field. The experimental set-up for fill Section II is shown in Figure 17 at the 75% fill level. Initially, the tests were conducted on the same fill levels as Design I, at the 0%, 25%, 50%, 75% and 100% fill levels. The fill level was then varied further from 0% to 100% based on the initial plotted results.

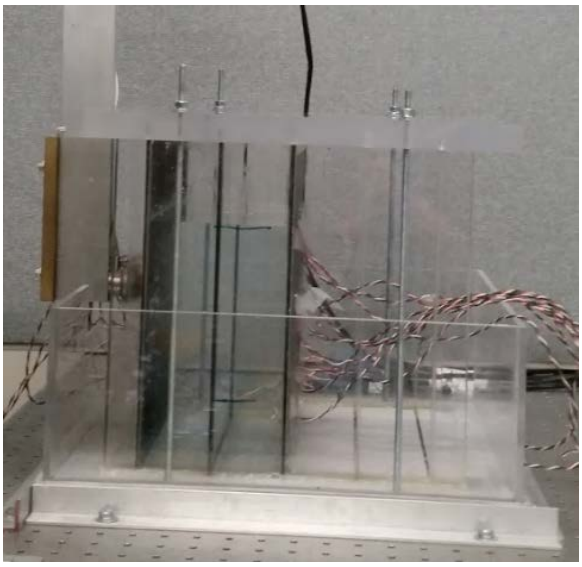

Figure 17. Experimental Set-up at Section II

The tests conducted on Section II were repeated for Sections I and IV. The objective of the research was to observe the behavior of the back plate and determine what effect the added water would have on the stress profile of the structure. The coupling effect between the two structures was analyzed at multiple sections and multiple fill levels to help determine critical design parameters. The impact force was also measured at all fill levels. The force was analyzed to determine the maximum magnitude of force, time to max magnitude and the contact duration on the plate and the impact device. A Fast Fourier Transform (FFT) was applied to the strain history data and the first excited frequency was recorded to determine the natural vibrational frequency of the plate. The strain during the Section II test was measured at all eighteen strain gauges. The strain for Sections I and IV were only measured on six gauges because the behavior was symmetric for the left and right sides of the plate. The strain gauges used for Sections I and IV testing can be seen in Figure 18. Once the strain behavior was analyzed at the individual fill sections, the data was compiled and plotted together to determine if there was any consistent behavior in the fluid coupling as the fill level increased, the distance between the structures increased or both.

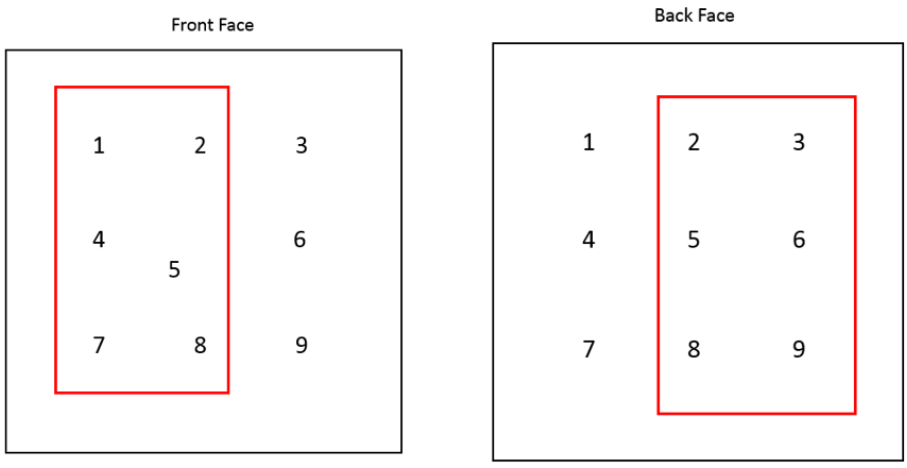

Figure 18. Gauges Used for Sections I and IV Testing

3. Fill Levels

The fill levels used for both Phase I and Phase II testing of Design I are shown in Table 2. The fill levels were chosen because they were the same as the previous research in order to replicate the tests conducted by South and Pentaleri [2], [16].

Table 2. Design I Fill Levels

First Design Fill Levels	
Fill Level (ml)	**Fill Level (%)**
0	0
4000	25
8000	50
12000	75
16000	100

Design II fill levels were calculated using three test sections as shown in Table 3. The design used 16 fill levels to better understand the behavior of the strain and maximum plate displacement.

Table 3. Design II Fill Levels

Design II Compartment Fill Levels			
Fill Level (%)	Section I (ml)	Section II (ml)	Section IV (ml)
0	0	0	0
10	500	1000	2000
15	750	1500	3000
20	1000	2000	4000
25	1200	2450	5000
30	1450	3000	6000
35	1700	3500	7000
45	2150	4500	9000
50	2400	4900	10000
55	2650	5400	11000
60	2900	5900	11900
75	3600	7350	14850
80	3850	7850	15850
90	4300	8800	17800
95	4550	9300	18800
100	4800	9800	19800

THIS PAGE INTENTIONALLY LEFT BLANK

III. ANALYSIS AND RESULTS

A. DESIGN I ANALYSIS

1. Force Analysis

The impact force data was collected for all runs and analyzed to compare the maximum amount of force being applied to the structure and the increase in force as the fill level increased. Ten tests at every fill level were compared to see if there were any inconsistencies in the magnitude of force for that particular level. As shown in Figure 19, the force was very consistent for the 75% fill level and the same results were achieved for all of the other fill levels. The force was similar for both Phase I and Phase II tests. The remaining figures used to determine consistency in test data were omitted from this report for simplicity.

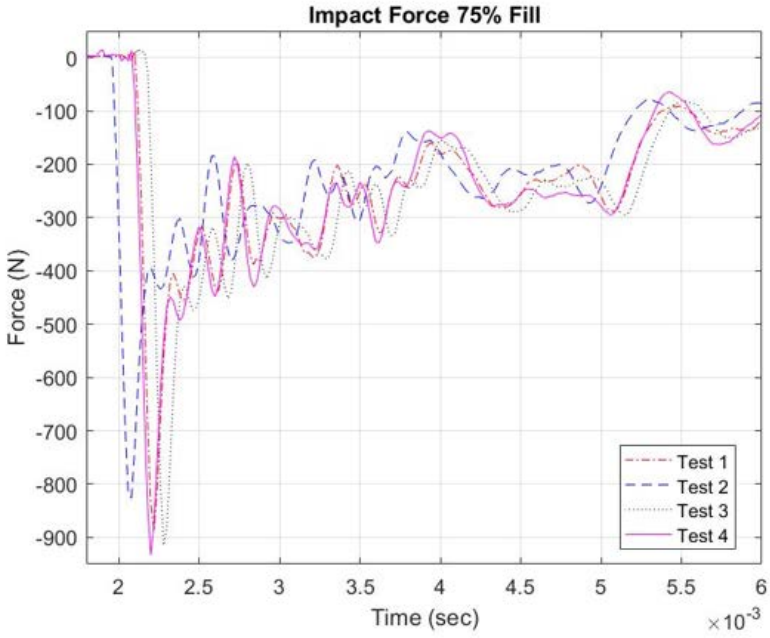

	Force_N
Test 1	-887.85
Test 2	-826.28
Test 3	-915.79
Test 4	-933.18

Figure 19. Impact Force at 75% Fill Level

The plot shows that after impact, the force oscillates until returning to zero. South [2] determined “the period of time that the force oscillated after reaching a maximum occurred because the cell was moving within its housing.” This phenomenon is common among force measuring devices due to the simple attachment point which hold the housing together. The oscillating behavior was also attributed to the recoil force the box exerts on the impact device. The added mass effect caused by increasing the volume is shown in Figure 20. The force was doubled as a result of the added mass effect due to the change in volume from the 25% fill to 50% fill level.

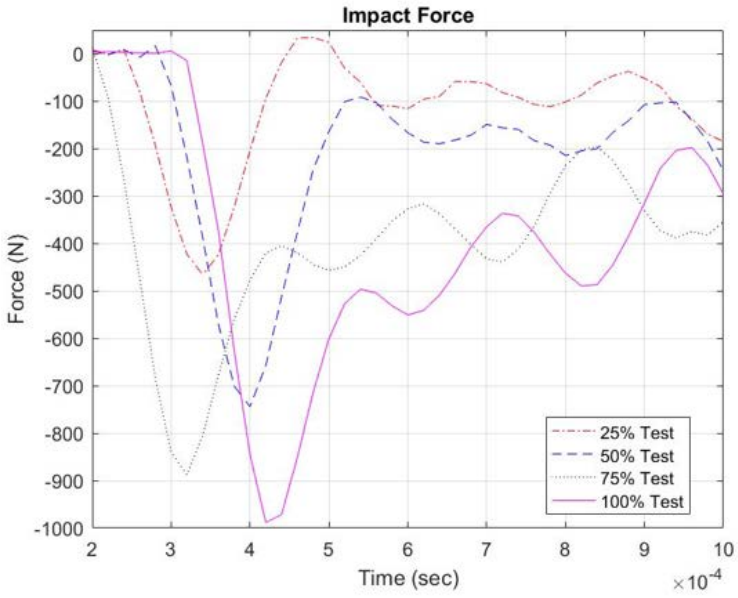

	Force_N
25% Fill	-465.65
50% Fill	-744
75% Fill	-887.85
100% Fill	-988.2

Figure 20. Impact Force for at all Fill Levels

The recoil, or force acted upon the impact device by the structure is plotted in Figure 21. The impact device made contact with the box and remained in contact for approximately 10msec prior to breaking contact. The force acted on the impactor is shown as the second increase in force on the plot. The period of time the impactor was in contact with the box depended directly on the fill level. The impactor remained in contact with the box for an additional 5msec for each increased fill level. The deformation and possible delamination of the front face of the box was studied extensively by South [2].

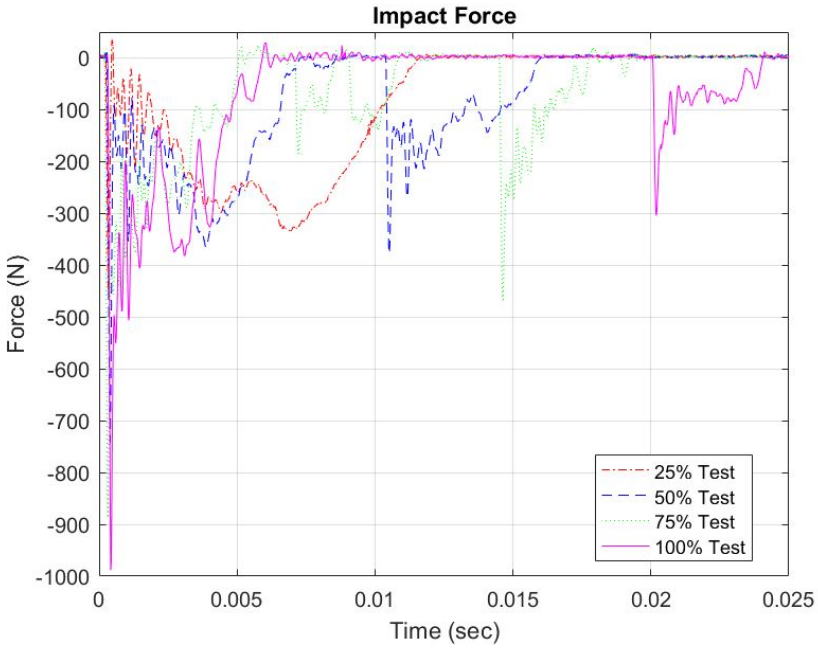

Figure 21. Total Impact Device Contact with Structure

2. Strain Analysis Phase I

Phase I strain testing focused on the strain magnitude measured with nine gauges. The data was recorded for a time-period of 50–70 msec depending on the fill level of the box. Ten tests were completed on all five of the fill levels. The magnitude of greatest strain did not always happen at the instant of impact but occurred as the force propagated through the water. An example of the accuracy of the data is shown in Figure 22. Four tests on the center strain gauge were compared at the 25% fill level. All nine gauges experienced the same repeatable results as shown in Figure 23. All tests maintained this precision and consistency, so all remaining figures show only one graph for simplicity.

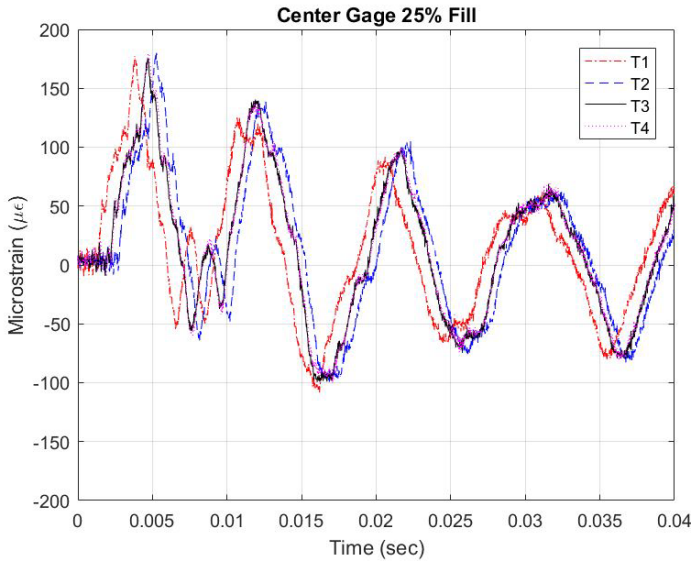

Figure 22. Test Case: 25% Fill Level, Center Gauge

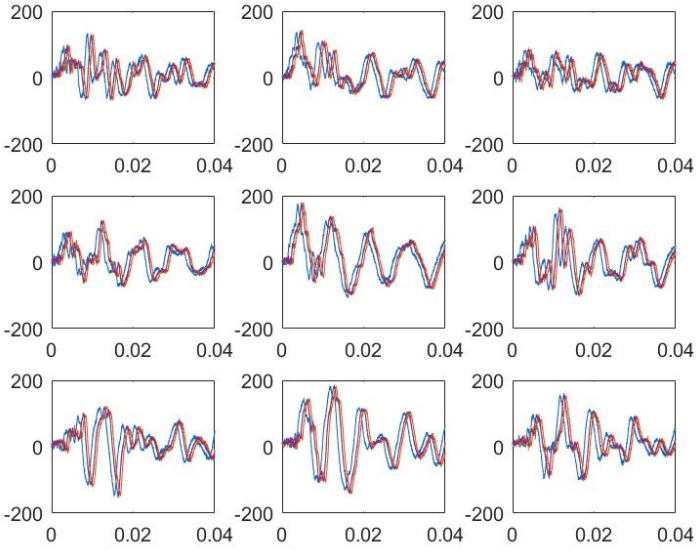

Figure 23. Test Case: 25% Fill Level, All Gauges

a. Strain Results: 0% and 25% Fill Cases

The maximum amount of strain for the 0% and 25% fill cases was much less than the strain on structures with larger volumes. As for the 0% fill case, the only strain measured was due to the vibration of the structure as shown in Figure 24. The 0% fill case was used as a normalization baseline to study the FSI effect due to the added mass of water. The numbers registered on Figures 24–28 are colored black for strain in tension and red for strain registered in compression. A bifurcation would show black and red numbers on the same line, but was not present in this study.

	Fill Level 0% (0mL)					
	Strain Results με					
Face Position	Test 1	Test 2	Test 3	Test 4	Test 5	Average Strain
1	16.5	15.9	16.6	16	13.8	15.76
2	12.6	18.5	13.5	11.7	12.4	13.74
3	19.7	17.5	20.7	18.3	17.8	18.8
4	12	12.5	13.7	11.6	11.7	12.3
5	14.6	16	13.8	13.1	13.5	14.2
6	13.6	16.3	13.2	14	10.8	13.58
7	14.8	13.2	14.3	14.4	14.2	14.18
8	12.3	13.4	12.3	12.2	14.3	12.9
9	30.1	32.9	27.3	30.2	32.5	30.6

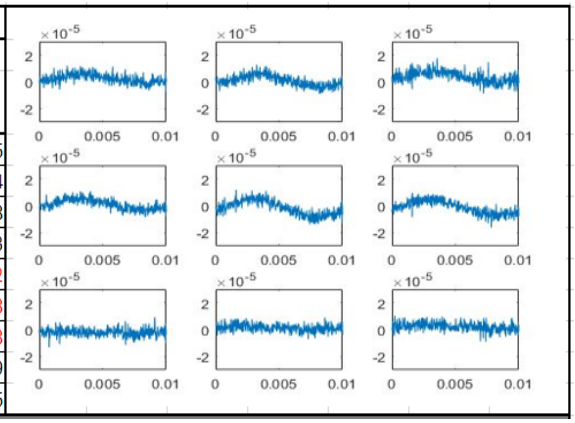

Figure 24. Strain for 0% Fill Case

The FSI effect began to influence the amount of strain on the structure as seen in the remaining cases. For the 25% fill case, the largest magnitude of strain on all gauges was in tension with the exception of Gauge 7. Gauge 7 is listed in red numbers and measured in compression for all five tests. All of the gauges oscillated while the added mass moved throughout the structure as shown in Figure 25. Of note, the average strain was calculated and listed on each of the fill case figures to show the increase in the magnitude with an increase in the water fill level.

	Fill Level 25% (4000mL)					
	Strain Results με					
Face Position	Test 1	Test 2	Test 3	Test 4	Test 5	Average Strain
1	133.6	130.8	123.8	130.3	120.3	127.76
2	137.9	143.2	136	142.3	132.1	138.3
3	83.5	85.9	92.2	86.5	88.3	87.28
4	102.6	127.2	126.3	125.9	129.9	122.38
5	177.3	180	176.1	180	170.5	176.78
6	146.5	159.1	167.1	160.6	155.9	157.84
7	149.1	148.3	147.6	153.2	143.6	148.36
8	182.4	182.2	181.4	186.3	177.4	181.94
9	157.3	155.3	154.1	161.8	149.6	155.62

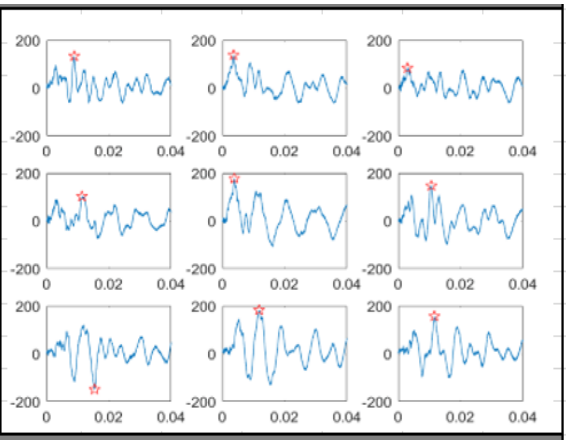

Figure 25. Strain for 25% Fill Case

b. Strain Results: 50% Fill Case

The 50% fill case in previous studies was the cause of the bifurcation and the main objective for Design I testing. Ten tests were conducted at this fill level attempting to replicate the bifurcation. The results of this case were similar to that of the 25% fill level, in that all of the gauges were in tension with the exception of Gauge 6, as shown in Figure 26. The maximum values of tension and compression are almost identical for face positions 1–3 and therefore did not produce a bifurcation. The gauges were below the water line and produced a minimal amount of strain. These tests were consistent with the tests conducted by Pentaleri, as the bifurcation was not prominent.

	Fill Level 50% (8000mL) Right Hold								
	Force Calculations		Strain Results με						
Face Position	Force Angle (deg)	Total Force	Test 1	Test 2	Test 3	Test 4	Test 5	Average Strain
1	45		126.2	117.5	117.3	116.3	118.9	119.24
2	45		189.3	170	180.7	169.5	170.2	175.94
3	45		145.5	131.4	142.7	128.7	132.6	136.18
4	45		192.8	172.1	195.2	167.8	171.8	179.94
5	45		210.4	199.2	223.8	192.2	171.2	199.36
6	45		143.2	145	163.2	151.1	166.2	153.74
7	45		242.4	257.8	242.4	236.3	225.5	240.88
8	45		248.4	224.1	256.6	258.4	230	243.50
9	45		192	193.7	194.7	189.3	181.9	190.32

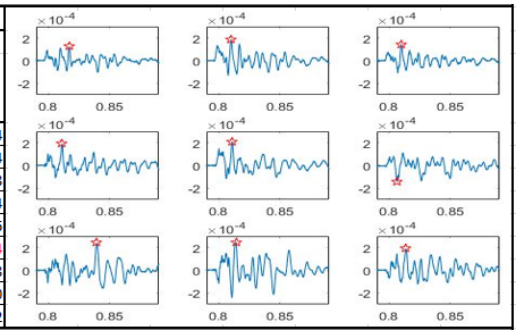

Figure 26. Strain for 50% Fill Case

c. Strain Results: 75% and 100% Fill Cases

The increase in strain was much more substantial for the top three gauges in the 75% and 100% fill cases. The change in strain from 25–50% was on the magnitude of 20 to 30 microns while the amount of strain on the back face at 100% full was double the amount at 50%. The 75% fill case was also the only case that did not register any strain in compression. Gauge 4 for the 100% fill case was the only gauge found in compression and this gauge remained in compression for all tests as this fill level. The results for both cases can be seen in Figures 27 and 28.

	Fill Level 75% (12000mL)					
	Strain Results με					
Face Position	Test 1	Test 2	Test 3	Test 4	Test 5	Average Strain
1	197.9	174	213.1	197.5	190.5	194.60
2	234.1	227.5	206.4	231.3	239.9	227.84
3	191.7	173.9	176.6	186.6	188.4	183.44
4	245	217.8	242.3	238.2	237.5	236.16
5	369.3	355.2	361.4	380.3	367.4	366.72
6	304.6	305.7	262.6	307.1	310.7	298.14
7	272	274.9	257.8	247.6	274.5	265.36
8	363.8	353.9	333.7	346.1	375.2	354.54
9	213.4	206	227.6	230.5	221.2	219.74

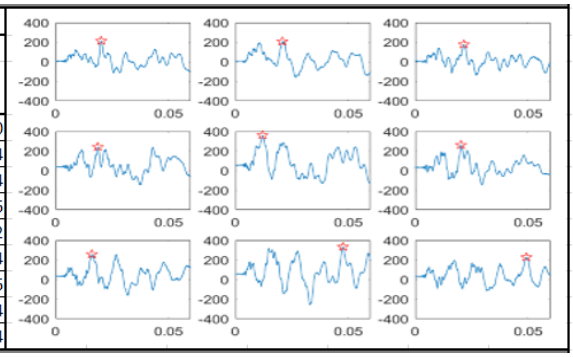

Figure 27. Strain for 75% Fill Case

	Fill Level 100% (16000mL)					
	Strain Results με					
Face Position	Test 1	Test 2	Test 3	Test 4	Test 5	Average Strain
1	277.7	256.3	254.5	276.4	260.5	265.08
2	448.4	449.7	457.6	458.8	468.2	456.54
3	338.4	324.5	317.8	327.1	303.7	322.30
4	274.3	290.4	289	267.4	285	281.22
5	517.9	493.8	481	496.7	475.3	492.94
6	223.6	210.5	215	203.8	227.6	216.10
7	357.5	342.7	330	358.7	318.3	341.44
8	507	483.4	480.3	488.2	498.6	491.50
9	324.7	321.2	304.5	305.5	306.6	312.50

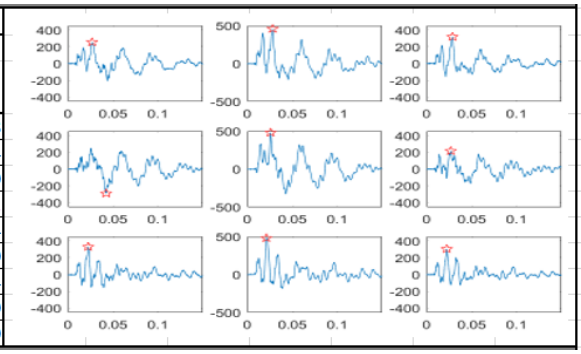

Figure 28. Strain for 100% Fill Case

3. Strain Analysis Phase II

The tests conducted during Phase II was only completed on the center strain gauge. The data was recorded for a time of 60 msec and ten tests were completed on all fill levels. The strain data comparison for four of the tests at the 50% and 75% fill levels can be seen in Figures 29 and 30. The data showed remarkable similarities to the data analyzed when using all nine gauges.

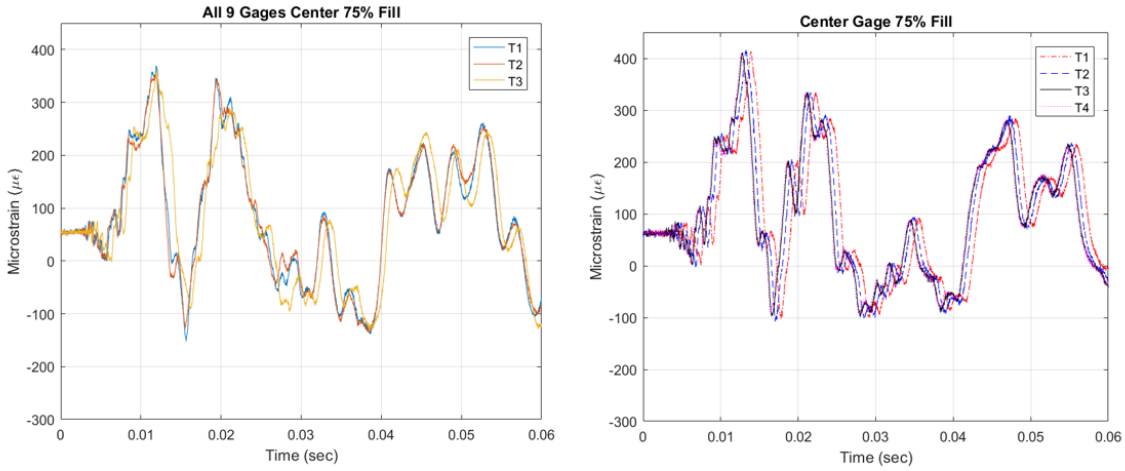

Figure 29. Strain Comparison at 75% Fill Level

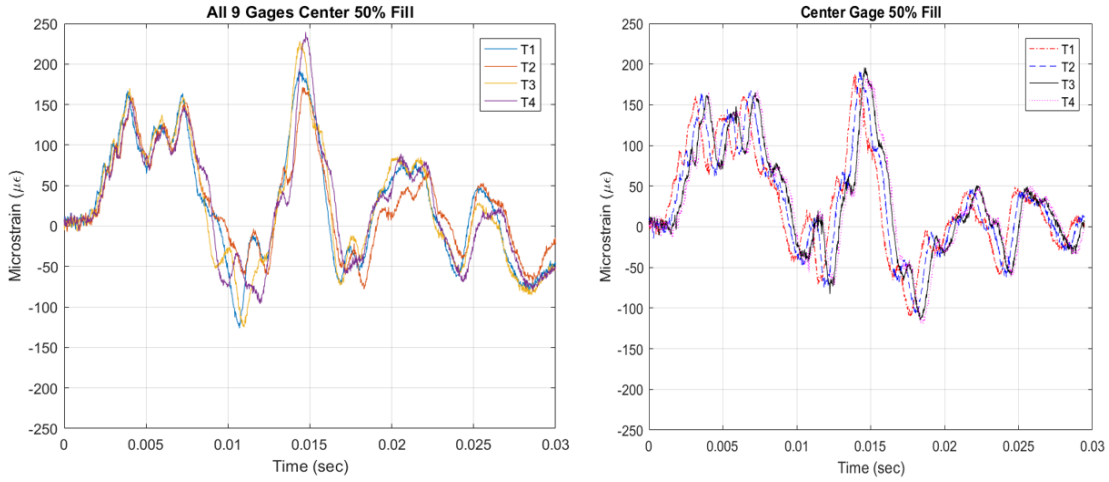

Figure 30. Strain Comparison at 50% Fill Level

Table 4 compares the data for maximum and minimum stress for the center gauge during Phase I and Phase II. For all cases, the maximum strain was in tension, and as experimentally proven, the bifurcation was not present.

Table 4. Strain Comparison between Phase I and Phase II

All9Gages =

	Ten	Com	Max
Test 1	191.96	-126.19	T
Test 2	171.27	-87.437	T
Test 3	228.29	-125	T
Test 4	239.46	-96.22	T

CenterOnly =

	Ten	Com	Max
Test 1	187.12	-110.78	T
Test 2	191.14	-108.73	T
Test 3	195.73	-115.23	T
Test 4	184.03	-119.25	T

B. DESIGN II ANALYSIS

1. Force Analysis

The impact force data was collected for all three fill sections at Design II and analyzed to determine the maximum amount of force being applied to the structure. The response of the force due to an increase in water fill and an increase in container size was also analyzed. The data was collected for ten tests at every section and plotted as a function of time at all water levels. The force for each section was then compared at the different water levels to see if there were any inconsistencies in the magnitude of force for that particular level. As shown in Figure 31, the force was very consistent for the 75% fill level. Similar results were achieved for all fill levels at each of the three test sections. The force time histories are shown in Figures 32–34 with the plots split between two figures for the multiple fill levels so the graphs are not overcrowded.

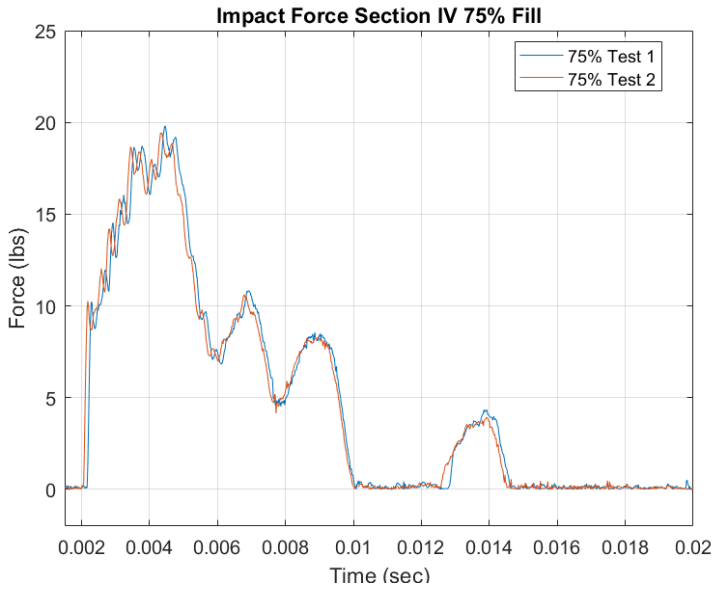

Figure 31. Impact Force at 75%

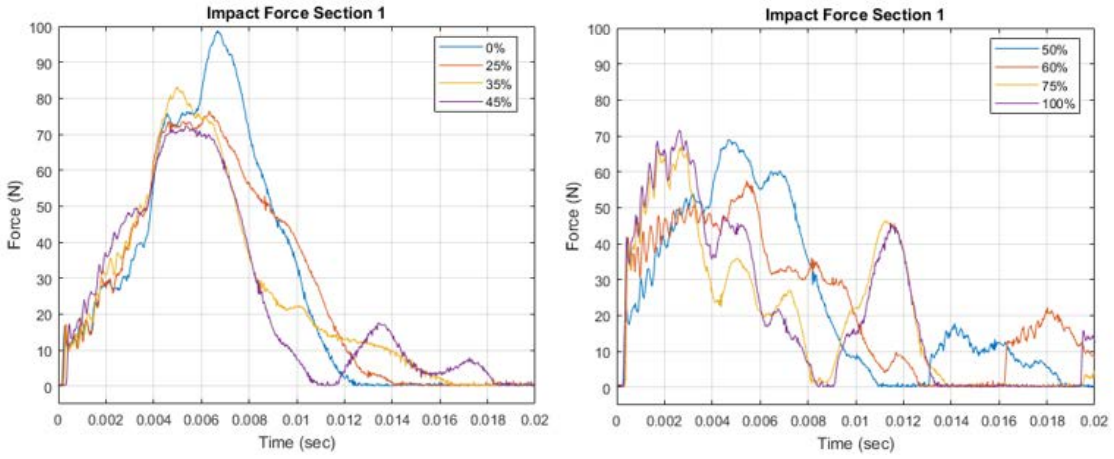

Figure 32. Impact Force Data at Section I

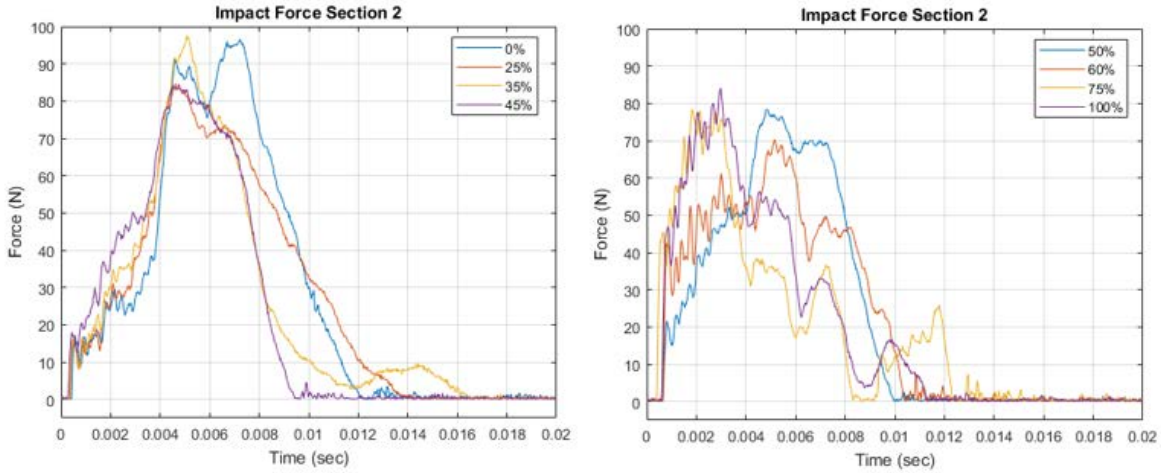

Figure 33. Impact Force Data at Section II

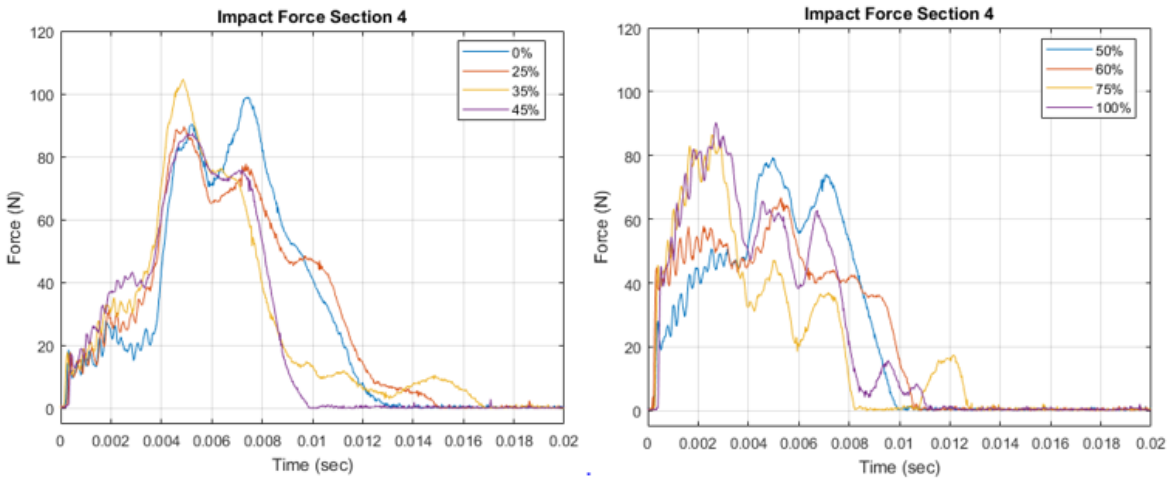

Figure 34. Impact Force Data at Section IV

There was no clear trend in the data for any of the fill sections, as the maximum impact force did not increase with fill level as expected. The peak force was consistently at the 0% and 35% fill levels for all sections. Of note, the lower water levels resulted in greater impact force than the higher water levels. The maximum peak remained very constant at water levels greater than 50% and with water levels above 75%, the maximum peaks look identical. The trend in the force verses water level was very similar for all three sections tested. As noted by South [2], the oscillations in force after the peak is attributed to the cell moving within the impact device housing.

The time to peak impact was also analyzed. As the water level increased, the time to reach the peak impact force decreased. The time to reach the peak force with no water was 0.007 sec. The time to reach peak force from 10% to 60% full was between 0.005 and 0.006 sec. When the fill level exceeded 75%, the time to reach the peak force was less than 0.003 sec. From the plots in Figures 32–34, the impact device was in contact with the structure for a longer period of time when the structure's water level was greater than 50%. The plate contact duration was much shorter and the force was much larger when no water was present and had a shorter impact time period.

Design I testing results showed that the force increased as a function of the water level on a solid structure. Design II proved that the force did not increase as a function of the water level for two separate structures. The maximum force was plotted against each fill level for all three sections in Figure 35.

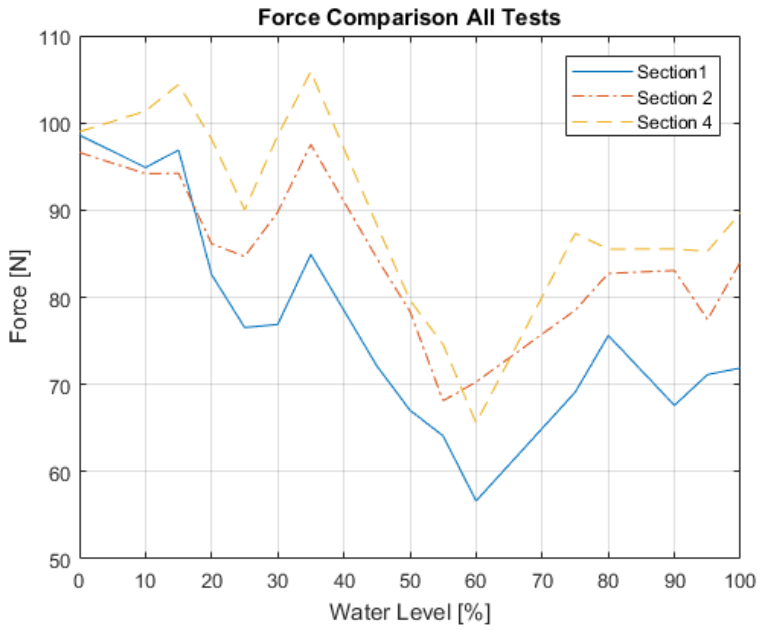

Figure 35. Impact Force Sections I, II and IV

The deformation in the plate increased with an increase in water level but the force did not, as the impact force can decrease while the deformation and water level increased. The next paragraph of this paper discusses the strain and deformation responses due to the added mass and FSI between the two plates. A numerical analysis was conducted using the displacement ratio of a mass-spring system to prove that the vibrational characteristics of the system play a key role in the deformation, and the force can decrease even with an increase in strain and displacement [10].

2. Strain Analysis

The objective of the strain analysis was to determine the fill level that caused the front and back plate to experience the maximum amount of strain and subsequent failure. The maximum amount of strain was correlated to the maximum amount of displacement and failure of the design. The PMMA and aluminum material that separated the two plates fully constrained the plates so they acted independently of one another. The strain was initially measured at the 0% fill level to verify the plates were fully constrained. The design apparatus was secured to the vibration table using L-brackets and screws. Initial testing showed strain being registered on the back face when the front plate was struck with the impact device. Prior to additional testing, the structure had to be fully constrained so the back plate would not register vibrations caused by the impact device.

To test the structure's rigidity, the strain was tested using four separate configurations to determine the needed level of constraint. The back-plate strain was measured with the top securing plate removed, the top placed on the structure without the securing rods to tighten it to the PMMA walls, the top secured to the walls with the rods and by placing brackets on the back side to add an additional constraint to remove vibrations. The strain was measured and compared for each level of improved stiffness. The strain was initially measured on Gauges 2, 4, 6 and 8 without the top PMMA plate attached and the plot is shown in Figure 36. The maximum values of strain were between 100 and 200 microns. The next three levels of security were also tested and the results can be seen in Figure 37. The strain magnitude was significantly higher when the top plate was attached to the structure. The strain when the top plate was secured with rods was identical

to the plot of strain with the rods and back braces. The last two constrained tests showed that the strain remained constant when the top plate was rigidly secured to the structure. For the remaining tests in the report, the top plate was rigidly connected with the rods tight. The back brackets were not used as they were deemed to be redundant. The registered amount of strain at the 0% fill level was used as a baseline and subtracted from all other water levels. The normalization was used to remove the stress that was transferred from the front plate to the back plate through the enclosed structure.

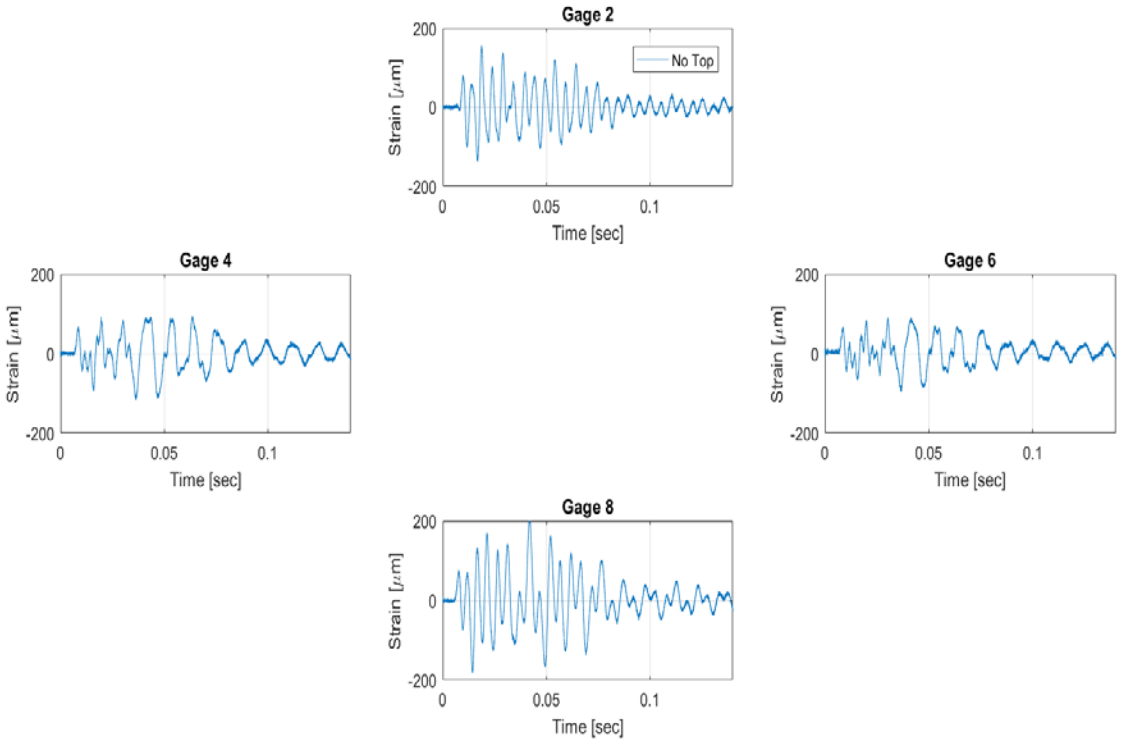

Figure 36. Strain without Top Securing Plate

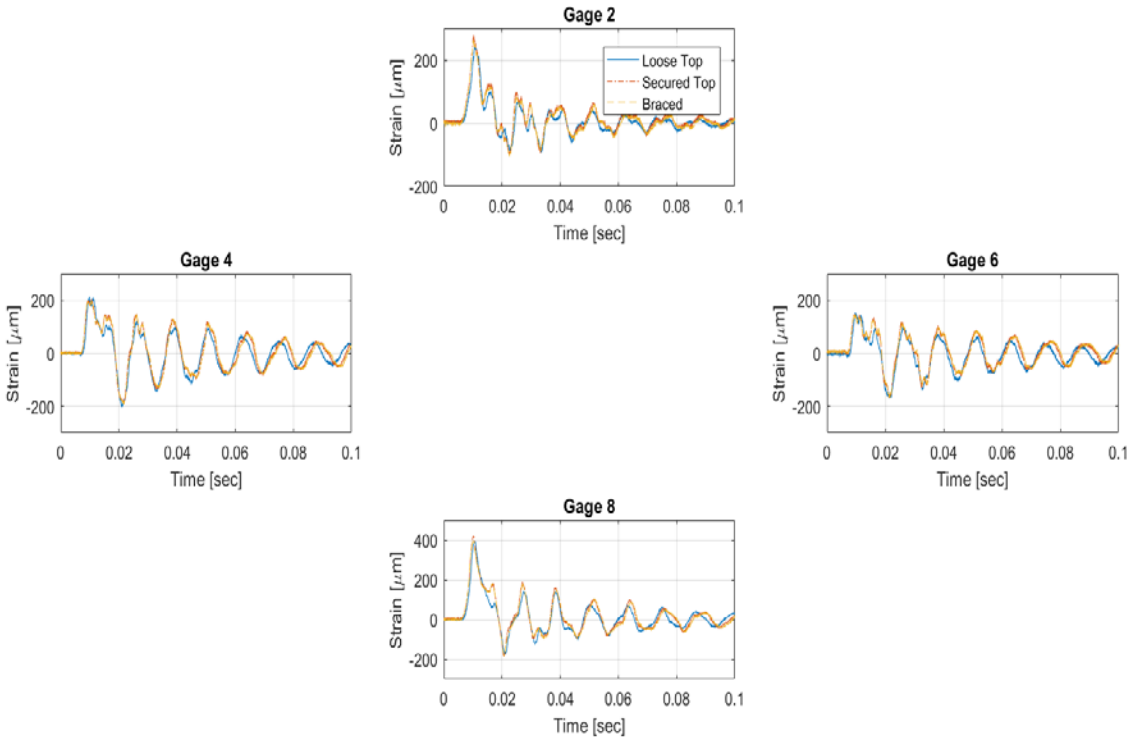

Figure 37. Strain with Constraints to Reduce Movement

Another issue when measuring the strain on the front and back face was sign convention. The strain gauges for both the front and back plate were outside the structure as seen in Figure 38. Once the impact device made contact with the front plate, it deformed and the gauges registered in compression while the back plate registered strain in tension. In order to give the strain gauges the same perspective, the sign of the front face gauges was changed during data analysis.

Figure 38. Plate and Strain Gauge Deformation

a. Strain Results: Section I

Fill Section I is the smallest section with the shortest distance between plates. The strain was measured on six strain gauges due to the symmetry of the plate and plotted against time and water fill percentage. Figure 39 shows the maximum strain on the front plate as it is plotted against the water level. The location of the strain gauges on the plate coincide with the 25%, 50% and 75% water fill levels. As shown in Figure 40, the registered strain was very minor until the water reached the 25% fill level. The gauges that did not fall below the water line were not greatly affected by the impact force. The largest amounts of strain on the front face registered at the higher water levels and were at the center gauges near the edges of the plate at Gauges 2, 4 and 8. Gauge 4 also registered two peak values. One peak was at 60% fill level while the other was at the 100% fill level. The gauges at the corners of the plate, Gauges 1 and 7, never registered a notable amount of strain. The increased water levels did not significantly affect these gauges.

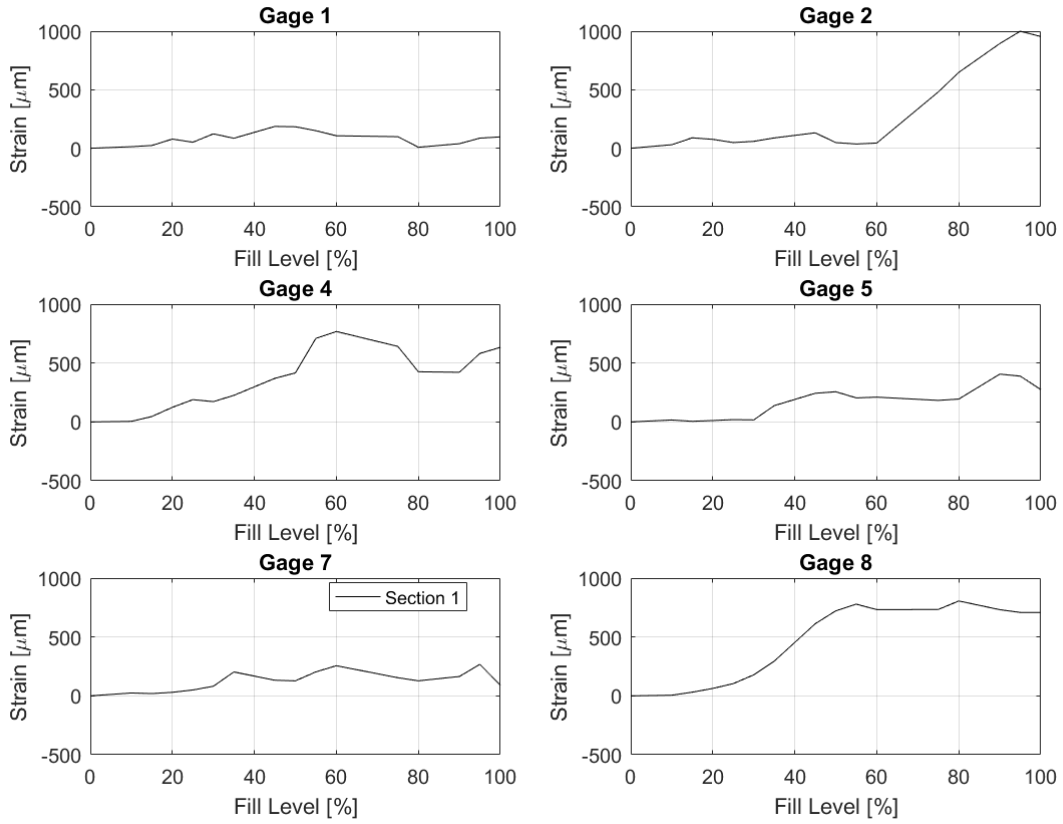

Figure 39. Section I Front Face Maximum Strain vs. Fill Level

The same phenomena can be said about the gauges on the back face as shown in Figure 40. The gauges did not register a significant amount of strain until the water level reached the height of the strain gauges. The largest amount of registered strain on the lower gauges was between the 35% and 60% water level and was lower at the higher water levels. Gauges 5 and 6 showed an increase in strain once the water level reached 50% but did not show significant peaks in the strain. Gauges 2 and 3 registered the largest amounts of strain once the water level was increased above 80%. Interestingly enough, the largest amount of strain on the structure was at the 95% fill level. When the structure was completely full, the maximum strain was lower. This phenomenon was repeatable for both Gauges 2 and 3. When the structure was completely full, the sloshing effect was negated and had an effect on the maximum strain levels. The results for both the front plate and back plate clearly show that the strain changes as a function of the water level.

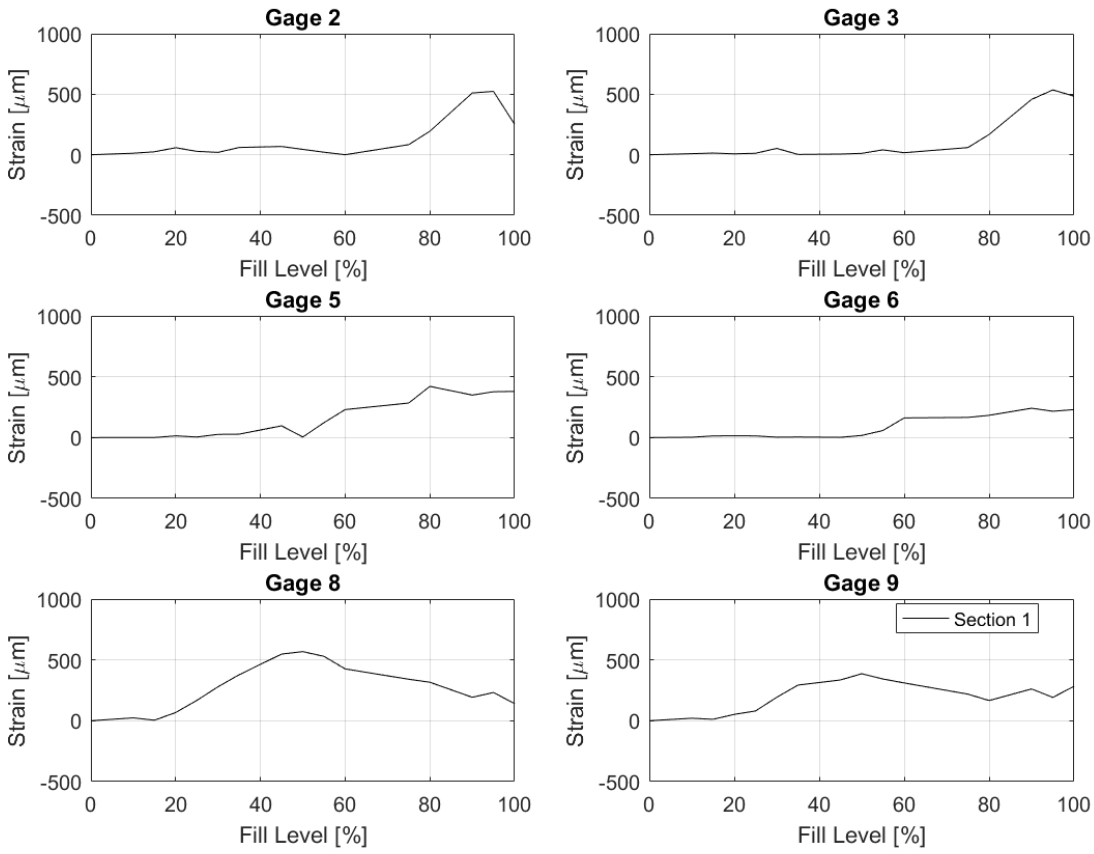

Figure 40. Section I Back Face Maximum Strain vs. Fill Level

The plots in Figures 39 and 40 are the normalized strain once the zero percent water level has been subtracted from the data. The registered strain without normalization at Gauges 2, 5 and 8 are plotted against time in Figure 41 at the 10%, 35% and 95% fill levels. Figure 41 gives perspective on the strain behavior as the water level increased. As expected, the registered strain for Gauge 2 was minor at the 10% and the 35% water level. The increase at Gauge 2 is shown at the 95% fill case once the water level reached the strain gauge. When the water level reached the strain gauges, they registered multiple peaks after the max peak. The strain gauges above the water surface had short periods of oscillation, while the gauges below the water line had multiple large peaks and large periods of oscillation.

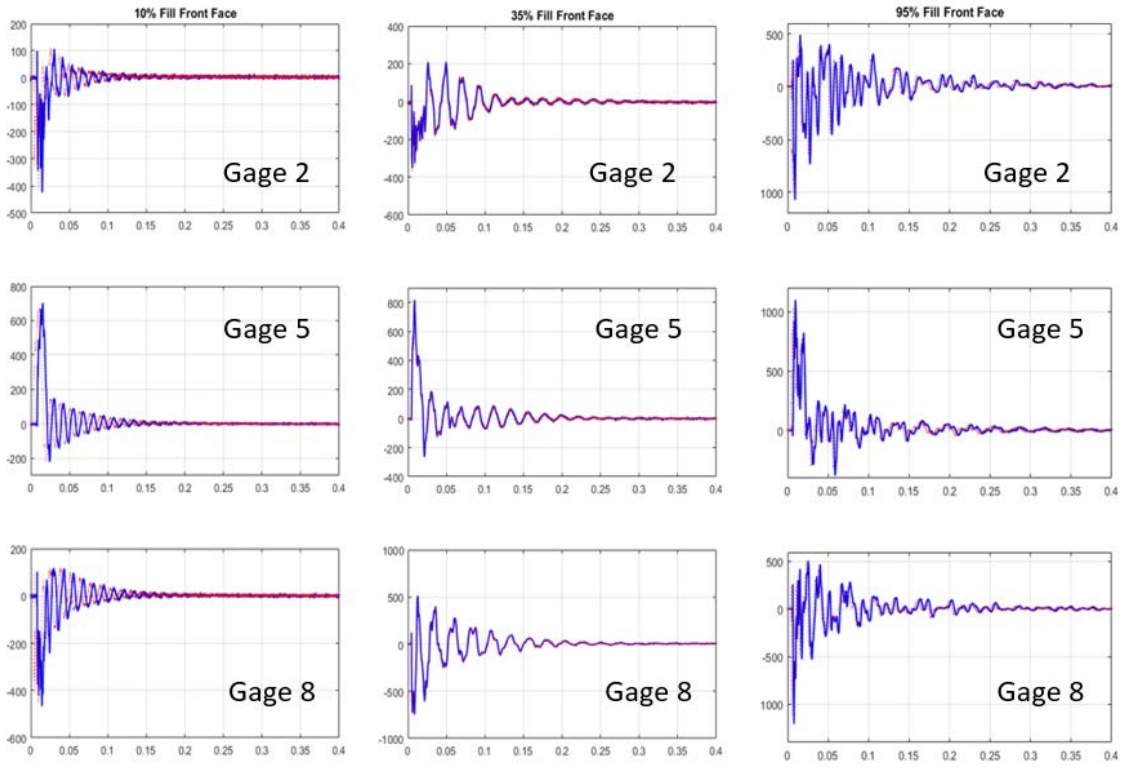

Figure 41. Registered Strain on Gauges 2, 5 and 8 at Three Fill Levels

b. Strain Results: Section II

Fill Section II was the first section tested. The data acquisition software used for testing had the ability to test 16 devices. During Section II testing, all nine gauges were tested on the back face, the impact device was used and five gauges were tested on the front face. The back face data was used to determine that the structure was symmetric as shown in Figure 42. The figure shows the left and right gauges combined for two separate water levels. All of the water levels returned similar results, so the tests for Sections I and IV were completed with 6 gauges on the front and back faces vice nine gauges.

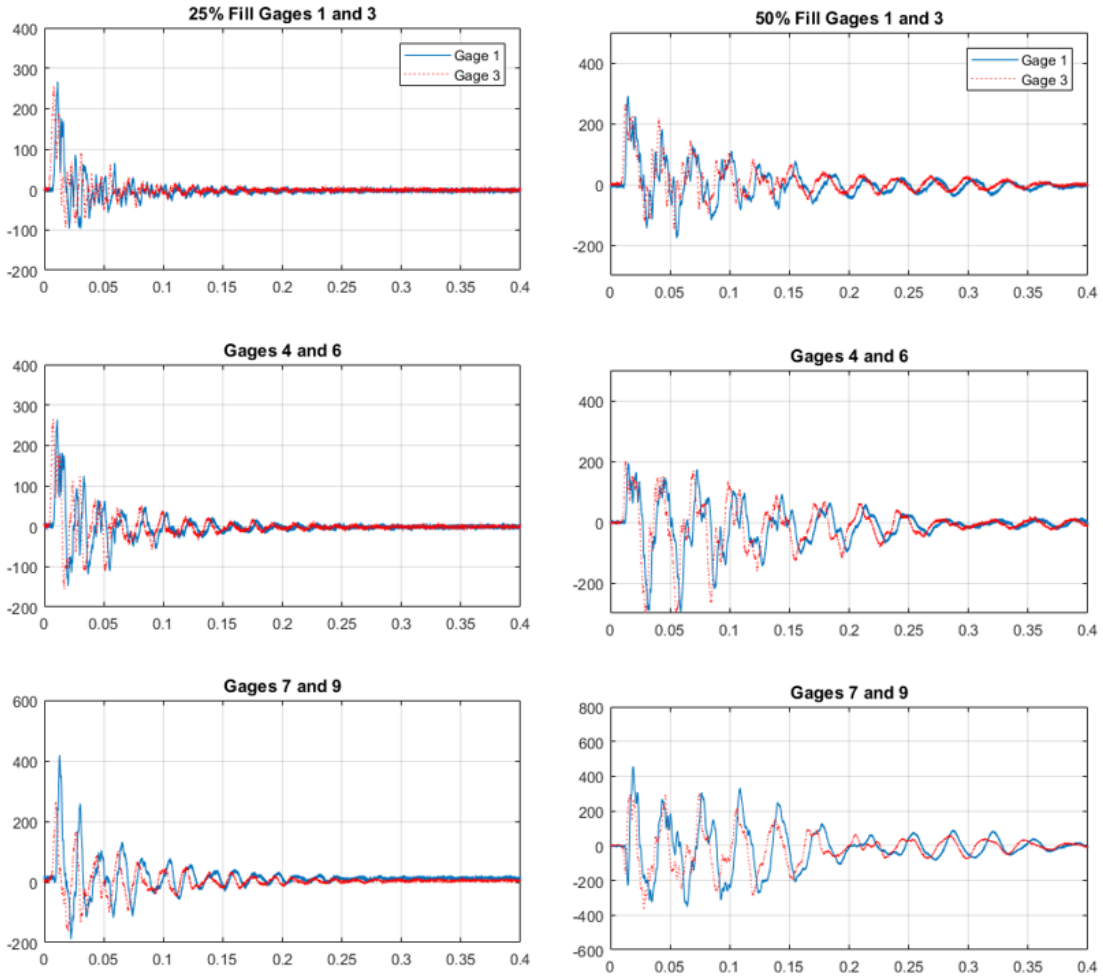

Figure 42. Back Plate Symmetric Gauge Data

Figure 43 shows the maximum strain on the front plate plotted as a function of the water level. As with Section I, the registered strain was very minor until the water reached the 25% fill level. The gauges above the water line registered very little strain in comparison to the gauges below the water line. The maximum amount of strain was in the middle of the plate at Gauges 2 and 8. Gauges 2 and 8 also showed the largest increase as the gauges fell below the water line. Gauge 4 had two peaks that were similar to the peaks at Section I. The first peak was at the 60% fill level with the second at the 100% level. Again, the results showed that the strain was largely influenced by the water level.

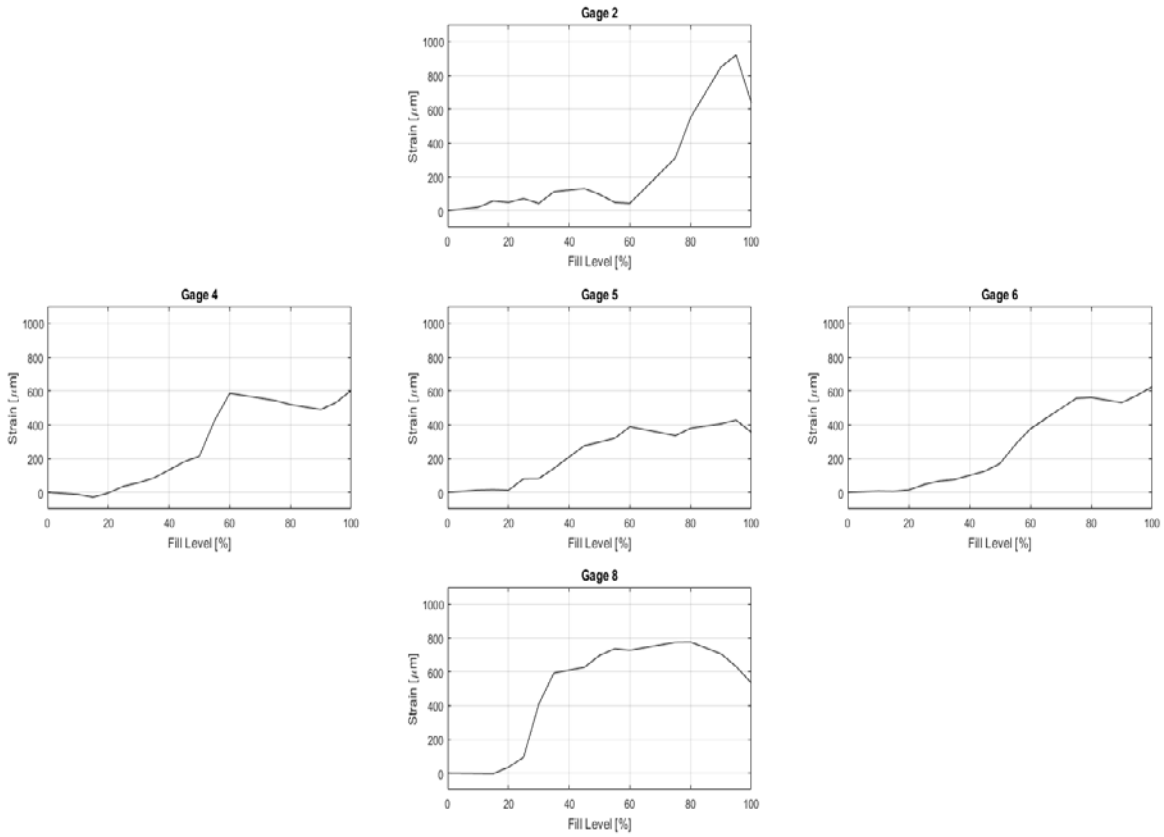

Figure 43. Section II Front Face Maximum Strain vs. Fill Level

The gauges on the back face of Section II showed very similar results to the back face of Section I as shown in Figure 44. All of the gauges registered very little strain until the gauges were below the water level. The largest amounts of strain were on Gauges 2 and 3 once the water level was increased above 80%. The largest amounts of strain on the structure was at the 95% fill level and when the structure was 100% full, the maximum strain level decreased as with Section I.

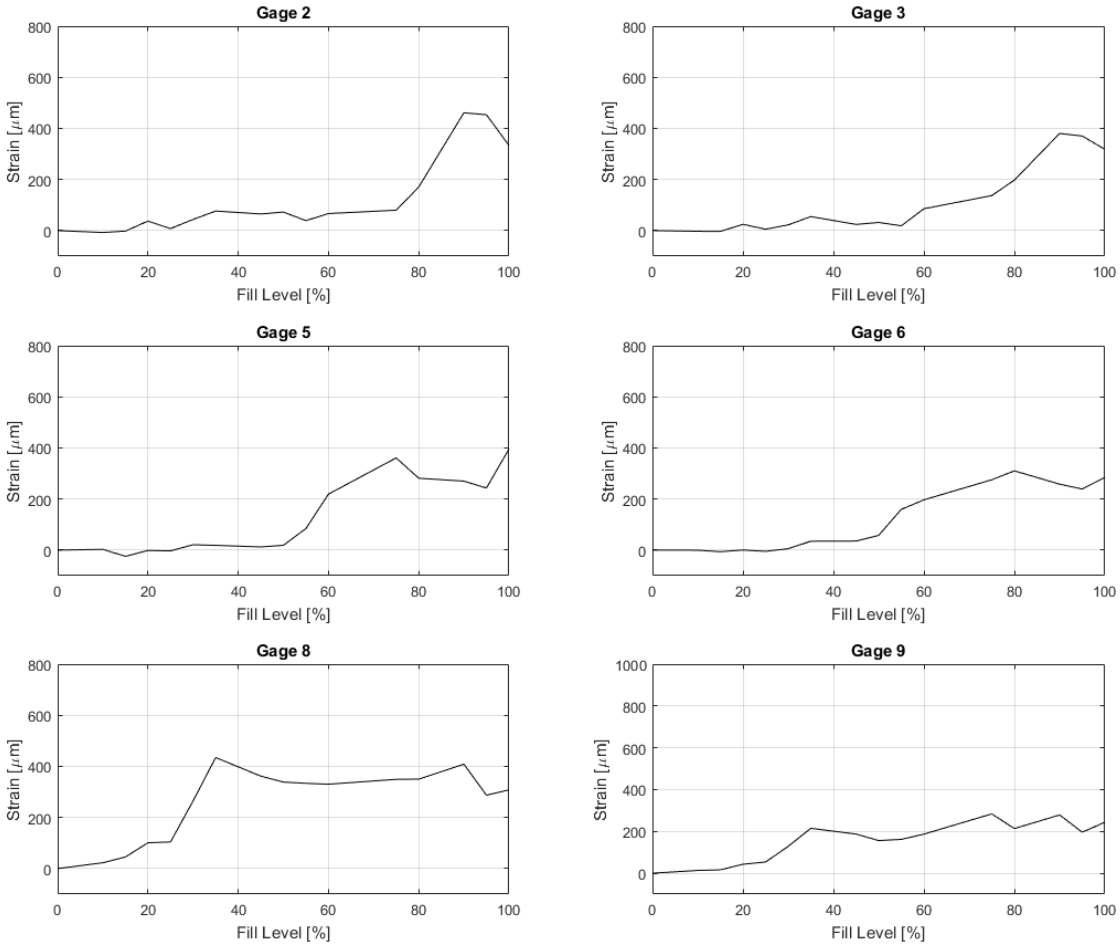

Figure 44. Section II Back Face Maximum Strain vs. Fill Level

c. Strain Results: Section IV

The results for Section IV are very similar to the previous sections. The water level continued to be the major determining factor in the strain registered on either the front or back face. On the front face, there were no new trends for this section as shown in Figure 45. Gauge 4 continued to have two major peaks and Gauges 2 and 8 registered the largest amounts of strain. The back face looked very similar to the results at Section II as shown in Figure 46. The similarities between Sections II and IV with no large increases from Section I was the determining factor in skipping Section III testing.

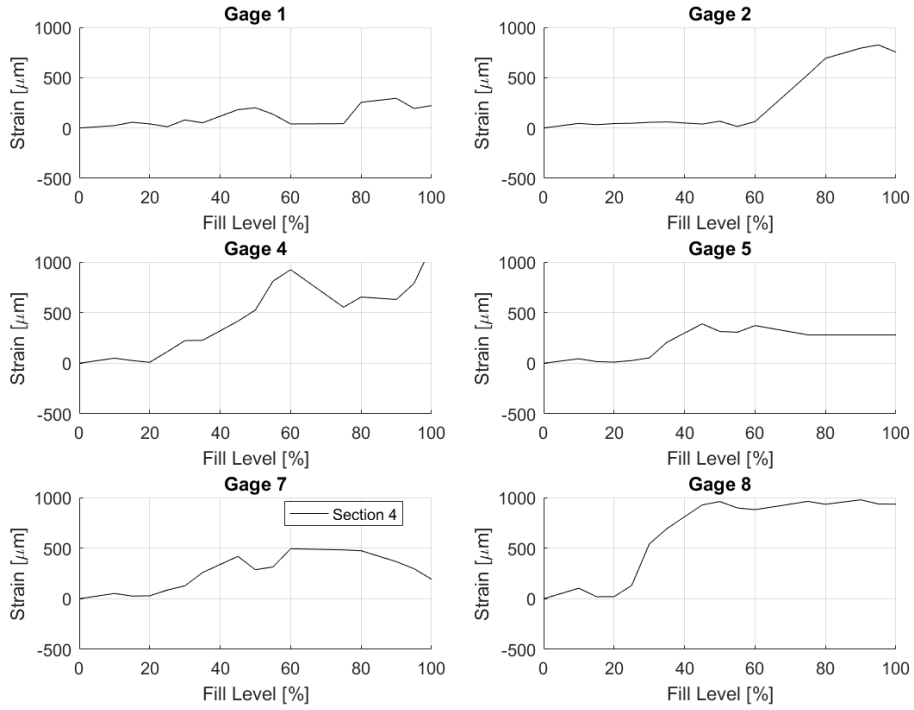

Figure 45. Section IV Front Face Maximum Strain vs. Fill Level

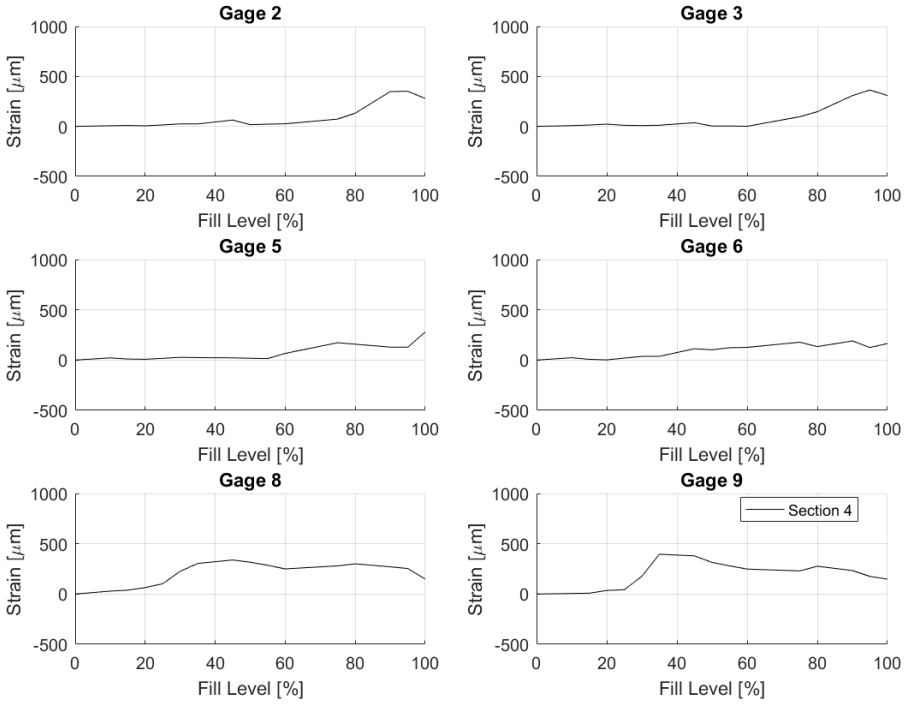

Figure 46. Section IV Back Face Maximum Strain vs. Fill Level

d. Strain Comparison

The strains for Sections I, II and IV had very similar profiles and were greatly influenced by the water level in the structure. The strain comparison gave the strain profile as it changed with the increased distance between sections. The front face strain, as a function of fill level, is shown for all three test sections in Figure 47. Gauges 4 and 8 have the largest strain at Section II. For Gauge 4, the maximum amount of strain was at the 60% fill level at 925 microns, which was 14% larger than the 800 microns for Sections I and IV.

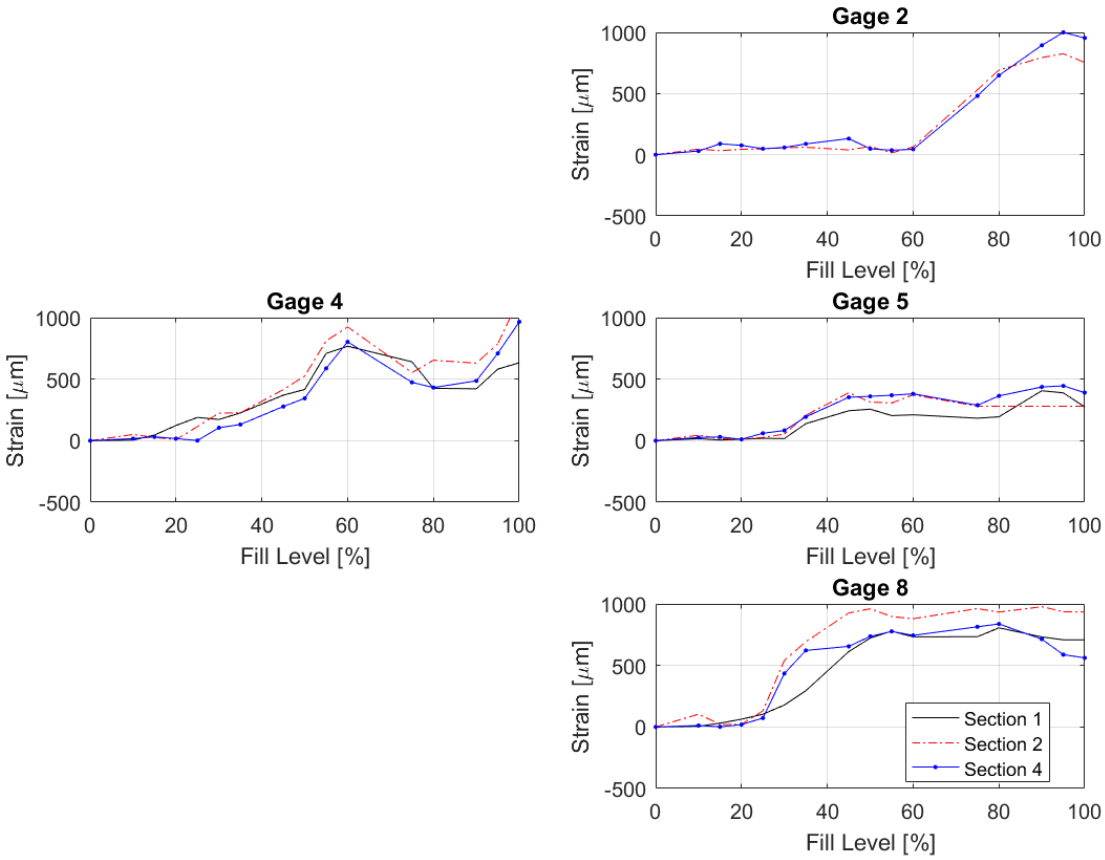

Figure 47. Front Face Comparison of Maximum Strain vs. Fill Level

On Gauge 8, each of the sections saw a large increase in strain at water levels greater than 25%. Section II had the maximum level of strain, with three peaks greater than 950 microns at the 50%, 75% and 90% fill levels as shown in Figure 48. At the 50% fill level on Gauge 8, the strain at Section II was 25% larger than the other two sections with an average overall strain increase of 15% at fill levels greater than 50%. At Gauge 2, the strain at the 95% water level was 17% higher at Section 4 than the other two sections. The distance contributed to the maximum levels of strain and Section IV had the largest level of strain when the structure was at the 100% fill level while Section II was the critical distance at the mid-fill ranges.

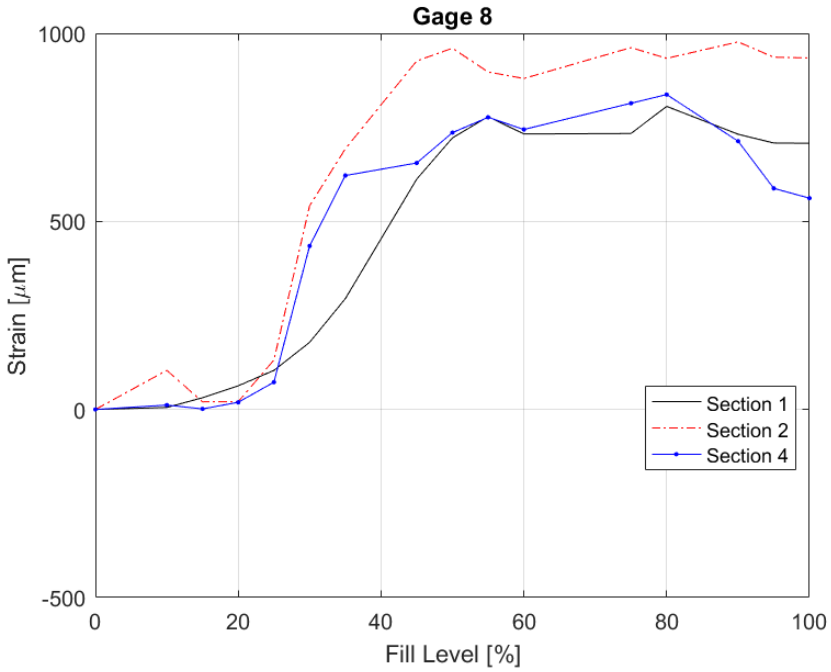

Figure 48. Front Face Gauge 8 Maximum Strain vs. Fill Level

The strain comparison for the back face maintained similar stress profiles to the front face as shown in Figure 49. Section I displayed the largest amount of strain at the high fill levels on Gauges 2 and 3 as well as the 35–60% fill level on Gauge 8. Similar to the front face, Section II had the largest amount of strain at center Gauges 5 and 6. The strain variations between sections was attributed to vibrational damping or viscous relationships between the fluid and the boundary layer on the side plates.

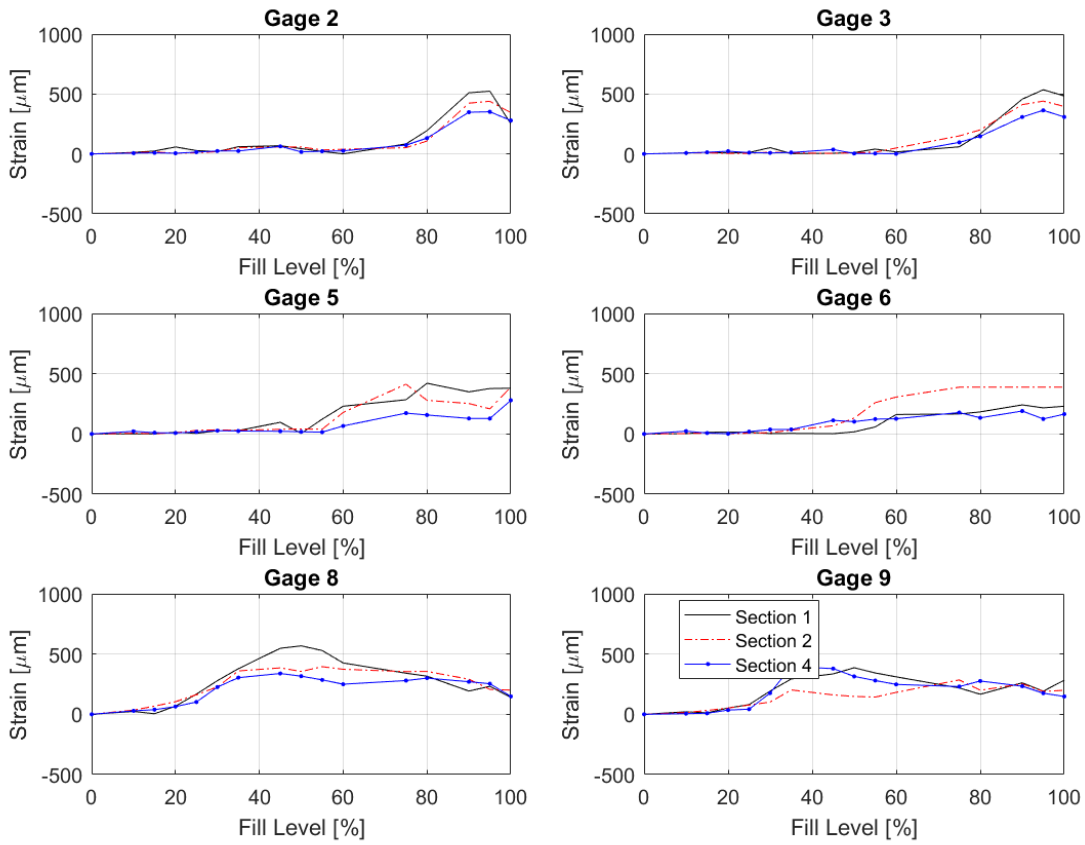

Figure 49. Back Face Comparison of Maximum Strain vs. Fill Level

The largest variation in back face strain was at Gauge 6 as shown in Figure 50. When the water levels exceeded 50%, the strain was significantly at Section II. The largest overall levels of strain were recorded at Section I at the mid-range fill levels and the upper gauges at the high water fill levels. All three sections proved to be critical in design criteria for multiple fill levels.

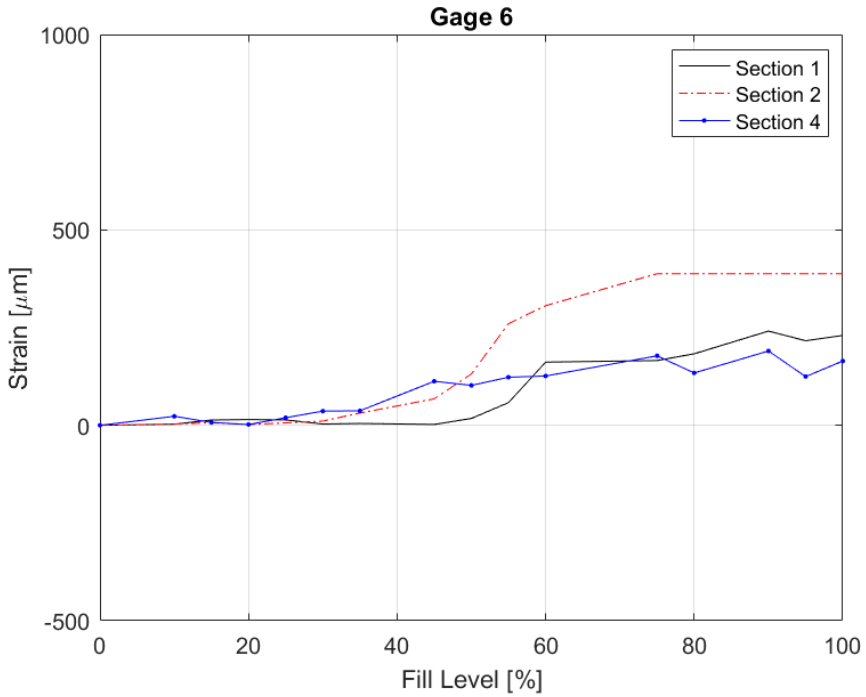

Figure 50. Back Face Gauge 6 Maximum Strain vs. Fill Level

3. Frequency Analysis

The vibrational frequency of the back plate was determined by applying a Fast Fourier Transform (FFT) to the strain history data of the plate. The first dominant excited frequency was recorded for all gauges on the front and back plate at every fill level. The change in the system's frequency was determined by the water fill level and the distance between the plates. The frequency was the same from the front plate to back plate during each individual test. The plotted log function varied from front to back plate, but the dominant excited frequency remained constant at a given fill level as seen in Table 5. As the water level increased, the first major frequency decreased.

Table 5. Back Plate Frequency Data (Hz) for Section I

SECTION I BACK FACE DATA												
0% Fill Level	Gage 2	76	10% Fill Level	Gage 2	76	15% Fill Level	Gage 2	72	20% Fill Level	Gage 2	66
	Gage 3	76		Gage 3	76		Gage 3	72		Gage 3	66
	Gage 5	76		Gage 5	76		Gage 5	72		Gage 5	66
	Gage 6	76		Gage 6	76		Gage 6	72		Gage 6	66
	Gage 8	76		Gage 8	76		Gage 8	72		Gage 8	66
	Gage 9	76		Gage 9	76		Gage 9	72		Gage 9	66

SECTION I BACK FACE DATA												
25% Fill Level	Gage 2	56	30% Fill Level	Gage 2	48	35% Fill Level	Gage 2	42	45% Fill Level	Gage 2	30
	Gage 3	56		Gage 3	48		Gage 3	42		Gage 3	30
	Gage 5	56		Gage 5	48		Gage 5	42		Gage 5	30
	Gage 6	56		Gage 6	48		Gage 6	42		Gage 6	30
	Gage 8	56		Gage 8	48		Gage 8	42		Gage 8	30
	Gage 9	56		Gage 9	48		Gage 9	42		Gage 9	30

SECTION I BACK FACE DATA												
50% Fill Level	Gage 2	28	55% Fill Level	Gage 2	24	60% Fill Level	Gage 2	22	75% Fill Level	Gage 2	20
	Gage 3	28		Gage 3	24		Gage 3	22		Gage 3	20
	Gage 5	28		Gage 5	24		Gage 5	22		Gage 5	20
	Gage 6	28		Gage 6	24		Gage 6	22		Gage 6	20
	Gage 8	28		Gage 8	24		Gage 8	22		Gage 8	20
	Gage 9	28		Gage 9	24		Gage 9	22		Gage 9	20

SECTION I BACK FACE DATA												
80% Fill Level	Gage 2	20	90% Fill Level	Gage 2	20	95% Fill Level	Gage 2	20	100% Fill Level	Gage 2	22
	Gage 3	20		Gage 3	20		Gage 3	20		Gage 3	22
	Gage 5	20		Gage 5	20		Gage 5	20		Gage 5	22
	Gage 6	20		Gage 6	20		Gage 6	20		Gage 6	22
	Gage 8	20		Gage 8	20		Gage 8	20		Gage 8	22
	Gage 9	20		Gage 9	20		Gage 9	20		Gage 9	22

Figure 51 shows the comparison between the front face and the back face frequency data at the 25% and the 50% fill levels for Section IV. As noted, the frequency profile is different, but the major frequency remains consistent for each plate.

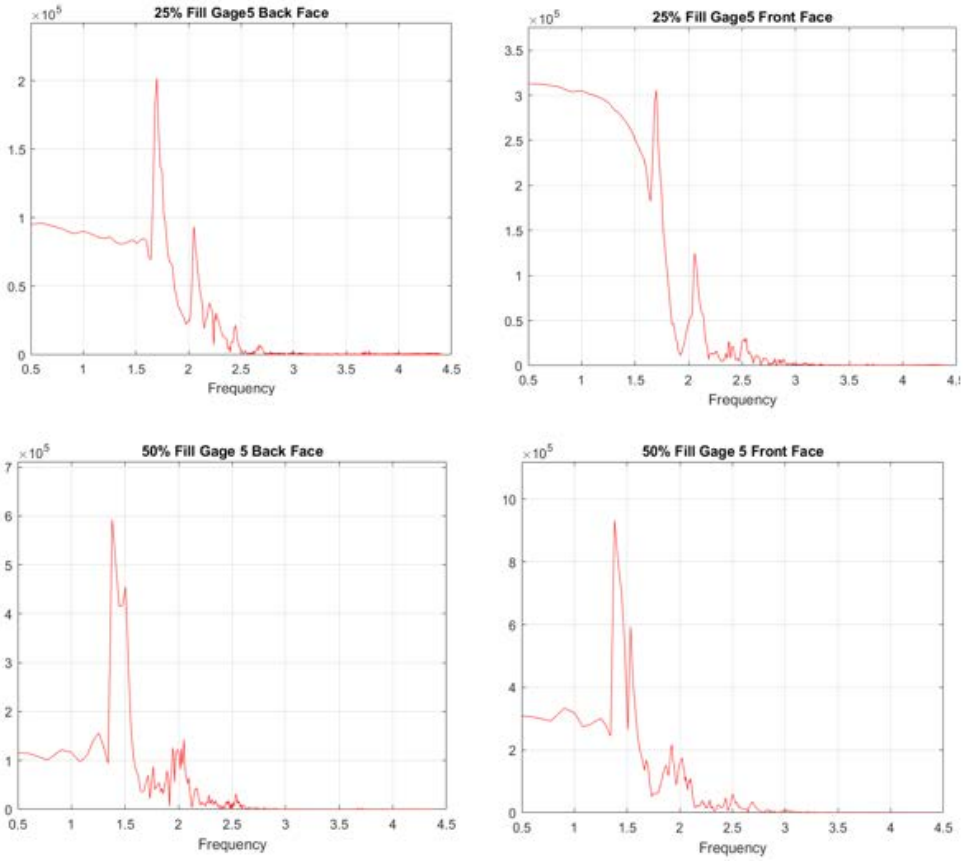

Figure 51. Dominant Frequency Comparison Front vs. Back Plate for Section IV

The magnitude of the dominant frequency also remained relatively consistent for all sections at a given fill level as shown in Figure 52. The excited frequency for the 50% fill level was 28Hz, 30Hz and 30Hz for Sections I, II and IV, respectively.

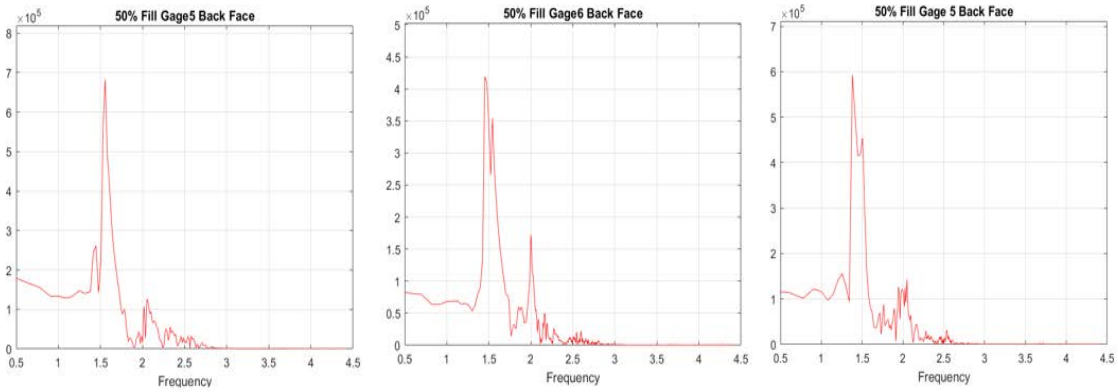

Figure 52. Dominant Frequency Comparison at 50% Fill for Sections I, II and IV

The frequency was normalized and plotted against the water fill levels from 0% to 100% as shown in Figures 53–55. The frequency decrease was attributed to the added mass effect of the water, which was a result of the FSI between the plates and the water level. Firouz-Abadi [12] stated that "the resonance frequency of a liquid filled tank will decrease with the increase of liquid density as well as the liquid depth in the tank." The frequency showed a linear reduction until the 50% fill level. Once at 50%, the reduction in magnitude tapered off and remained relatively constant at fill levels greater than 70%. The slight increase in frequency at the 95–100% fill level was attributed to the lack of a free surface to account for the sloshing effect of the water. This boundary condition constrains the water in all directions and caused a slight increase in the magnitude of the frequency. The change in frequency between the 60% fill level and the 100% fill level is very minor and was not investigated any further.

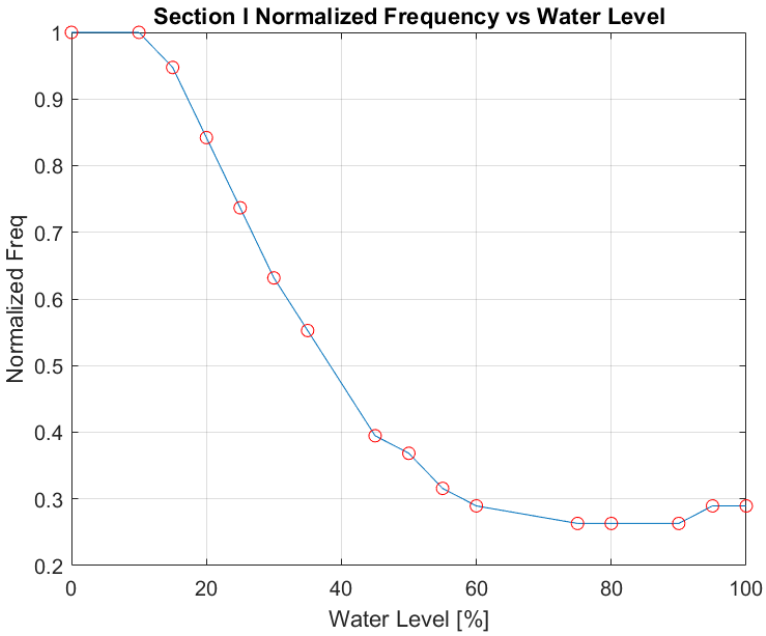

Figure 53. Normalized Plate Frequency vs. Water Level Section I

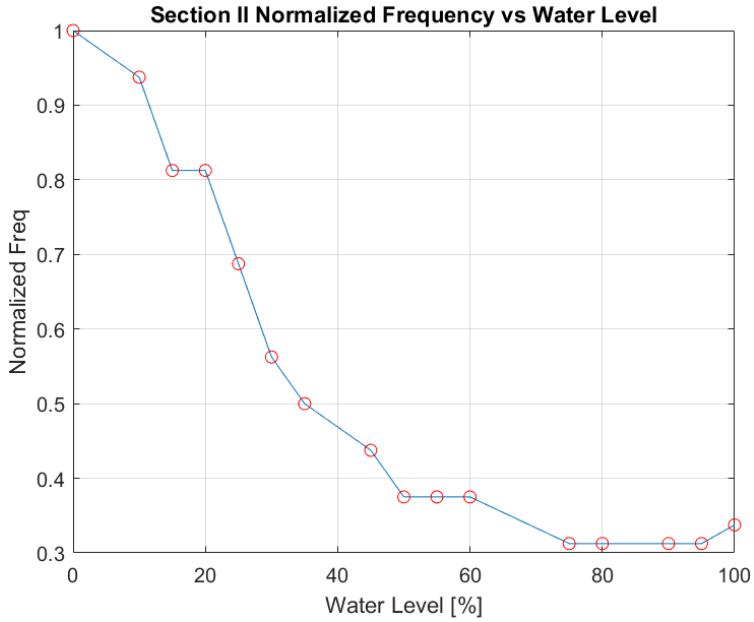

Figure 54. Normalized Plate Frequency vs. Water Level Section II

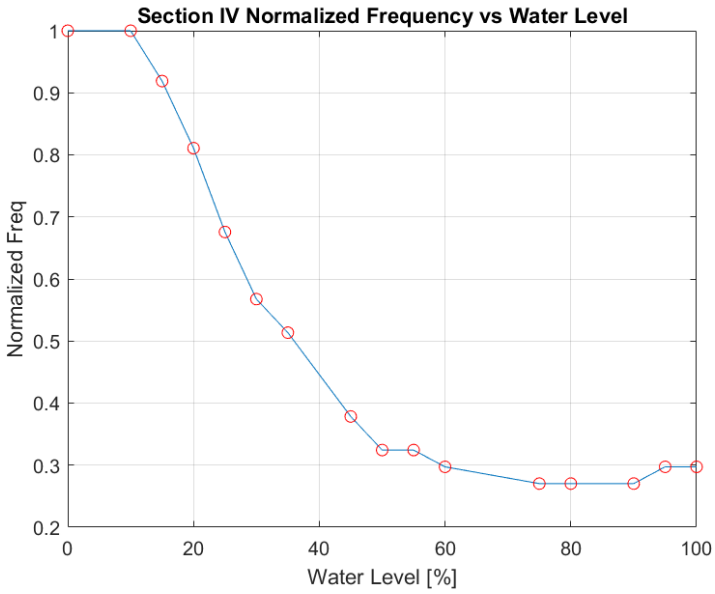

Figure 55. Normalized Plate Frequency vs. Water Level Section IV

IV. CONCLUSION AND RECOMMENDATIONS

A. CONCLUSION

This experiment was designed to study the fluid coupling that is caused by the FSI through a fluid medium between two structures, initiated by a low-velocity impact. A structure was fabricated with multiple compartments filled with a fluid used to simulate separate structures with a fluid medium between them. The dynamic response was transferred from the front plate to the back plate through the fluid medium. The FSI and water fill levels played a significant role in the stress response on both the front and back composite plates of the apparatus.

The impact force was measured with a load cell, attached to a swinging pendulum and released at a 45-degree angle. The impact force did not increase as a function of the water level, nor did the impact force present any clear trends in the data for individual fill sections. However, the impact force data was consistent and repeatable for all fill sections. The peak force was consistently at the 0% and 35% fill levels and the impact force was lower for the higher fill levels. When the water level was above 75%, the plots for all sections looked identical. The impact device's contact duration was longer when the structure water level was greater than 50%. Maximum strain and deformation occurred for larger volumes of water, not at the maximum impact force.

The strain response varied significantly with the water level. An increase in water level was directly proportional to an increase in strain. The strain on the front face was significantly larger on the center edges of the plate. The lowest amounts of strain for the front face was at the center and at the corners of the plate. The increase in strain was directly proportional to the water fill level and the distance between the structures. The maximum strain response on the front face was at the 95% fill level on the top center gauge at Section IV. The strain response on the back plate was very similar to the front face but the maximum strain level was at Section I. The strain on the back plate was also directly proportional to the water fill level. The strain was significantly increased when the water level was greater than 75%. The maximum strain response on the back plate was at the

95% fill level on the top center gauge. An interesting note is the decrease in strain associated with the 100% fill level. The added boundary condition caused the strain to be slightly less when the structure was completely full.

The frequency response of the structure was measured and it was found that the first major frequency decreased with an increase in water level. The frequency response was the same for the front and back plates. The frequency profiles varied slightly for each section, but the major frequencies remained consistent for all three fill sections. The frequency decrease was attributed to the added mass effect of the water as a result of the FSI. The slight rise in the frequency at the 100% fill level corresponded to the decrease in strain at that fill level. Both of these phenomena were a characteristic of the lack of free surface vibrations at the 100% fill level.

In conclusion, the fluid coupling effect between two structures is a significant design characteristic for engineers to consider. The strain did increase appreciably with an increase in water level. The distance between structures was also found to be a significant factor in the strain, but did not produce consistent results. The increase in strain resulting from the increase in distance was not as predictable as the increase in strain due to the fill level. These design characteristics must be taken into consideration when approaching an engineering problem that requires these types of loading parameters. Experimental testing will be crucial to determine the appropriate distance and water fill levels needed to meet the designs requirements.

B. RECOMMENDATIONS

Continued research parameters for this topic are based on altering the design parameters. The impact pendulum can swing up to a 90-degree arc to allow for an increased velocity. The pendulum also has a small weight block attached to it that can be altered to increase or decrease the impact velocity. The most critical design parameter is the plate thickness. The slots in the design structure allow for different thicknesses to be used in research. The plate thickness can be altered to determine a critical thickness for design based on the current dimensions. Different fluids can also be studied to analyze the effect the fluid density has on the results.

APPENDIX. PROJECT DETAILS

A. DESIGN CAD DRAWINGS

The structural parts were designed using PTC's Creo Parametric 3.0 student edition. The dimensions for the composite sheet and attachment rods were given in the report.

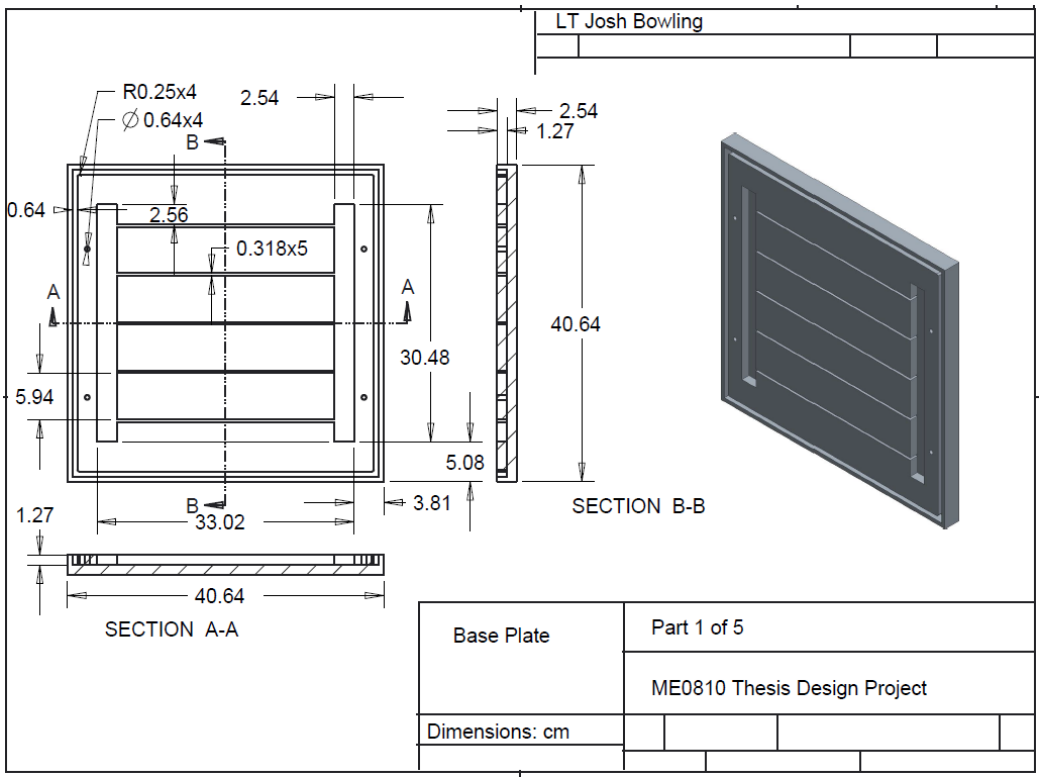

Figure 56. Base Plate CAD Drawing

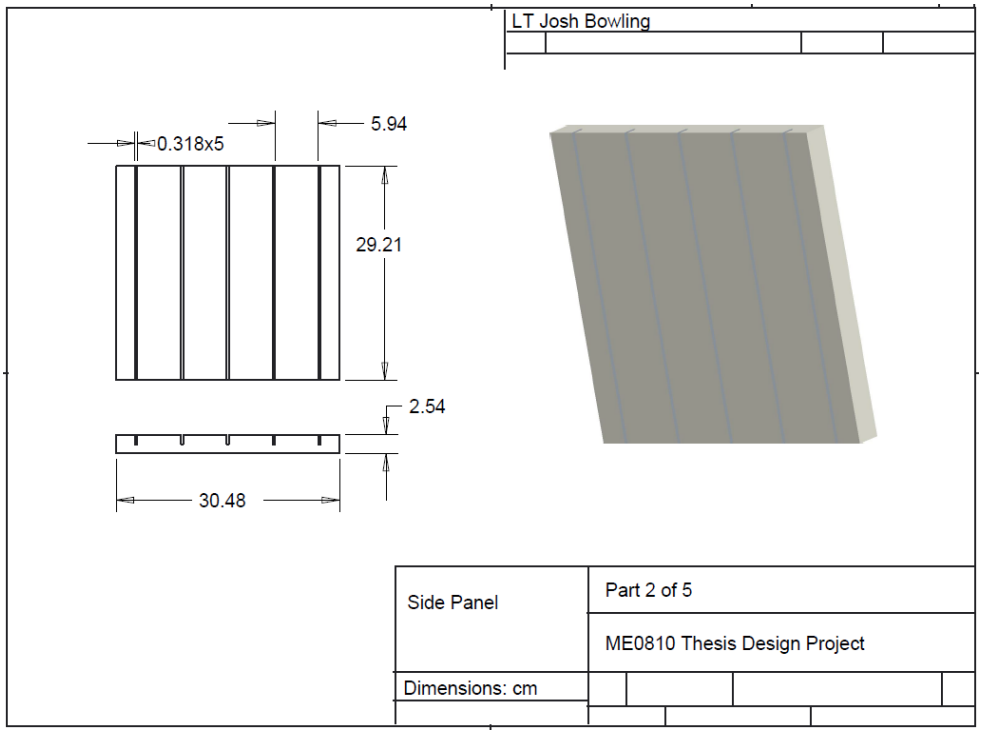

Figure 57. Side Plate CAD Drawing

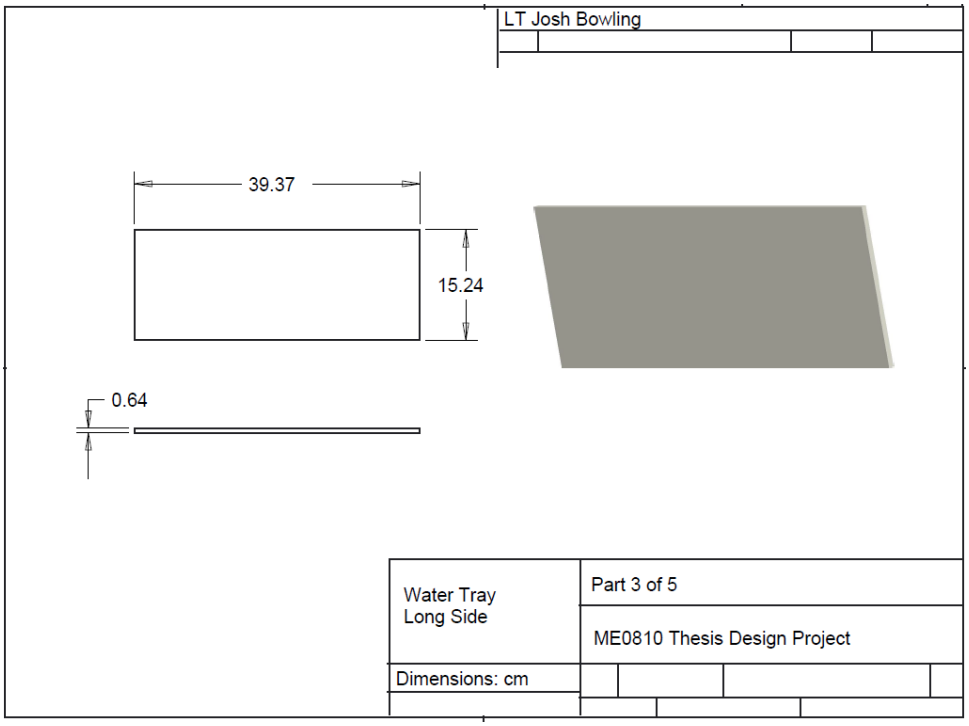

Figure 58. Long Tray CAD Drawing

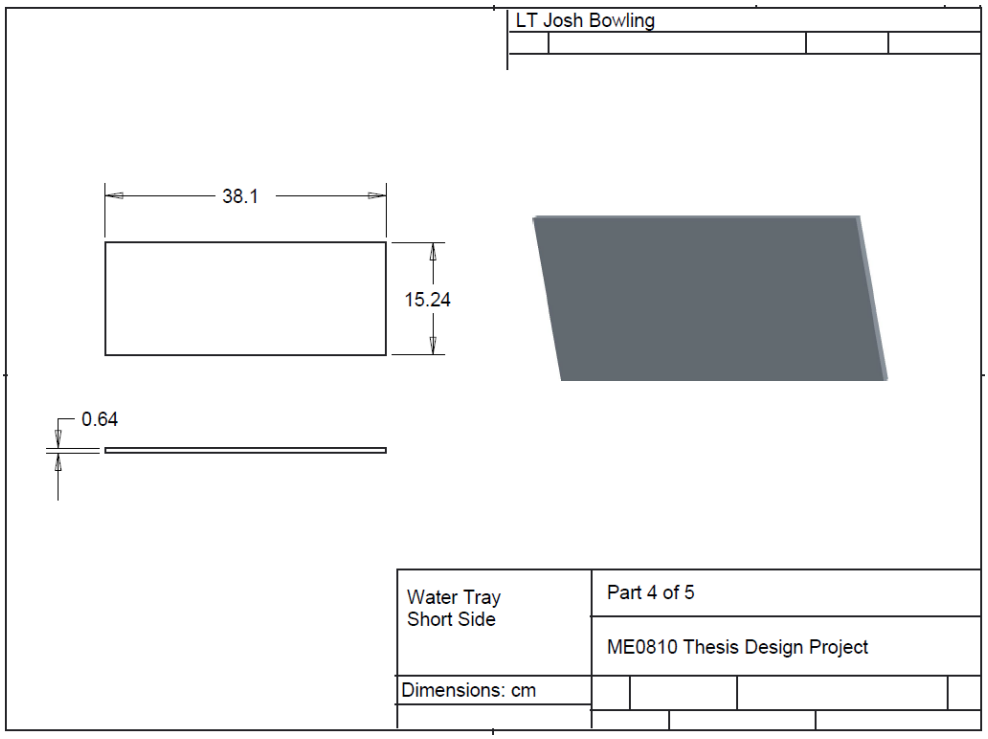

Figure 59. Short Tray CAD Drawing

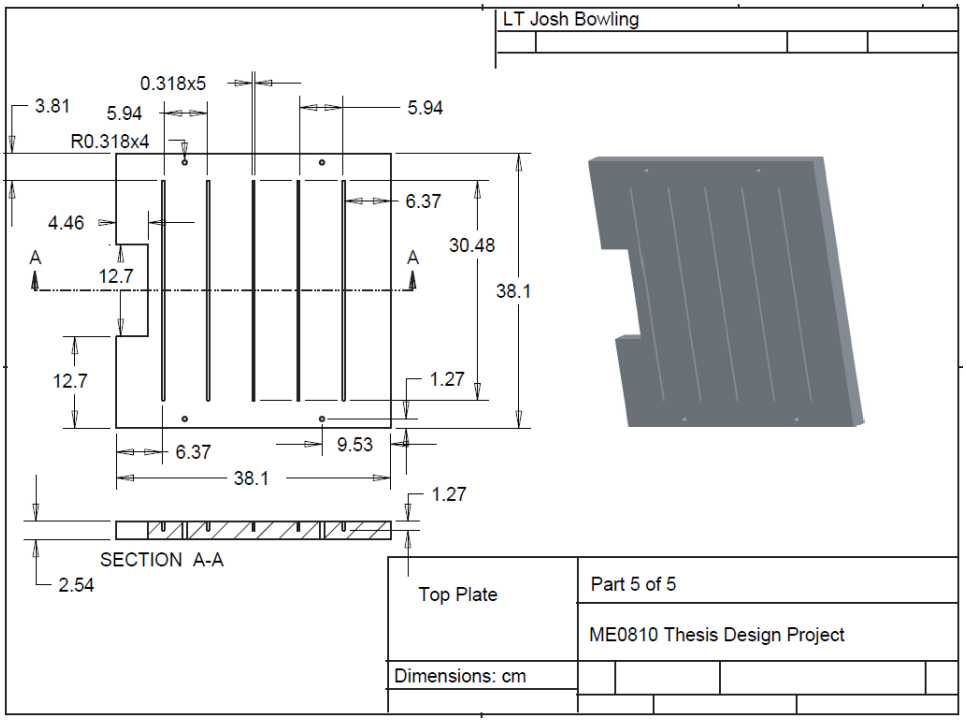

Figure 60. Top Plate CAD Drawing

B. DATA ACQUISITION DETAILS

1. Wiring Instructions

The strain gauge wires were soldered into place and connected to a Quarter-Bridge, NI-9945 screw terminal adaptor.

Figure 61. Strain Gauge Wire Placement

Figure 62. Strain Gauge Wire Lead Connection

The load cell wire leads were connected to a Force-Bridge, NI-9949 screw terminal adaptor. The location of the wires and their significance can be seen in Table 6.

Figure 63. Impact Force Wire Lead Connection

Table 6. Data Acquisition Wire Placement

Wire Placement		
Force Bridge (NI-9949)		
Terminal Number	**Wire Lead**	**Wire Designator**
1	Dark Green	Jumper (2)
2	Dark Green / White	Jumper (1) / (+) Output
3	Light Green	(-) Output
4	Not Used	Not Used
5	Not Used	Not Used
6	Red	(+) Excitation
7	Dark Green	Jumper (10)
8	Not Used	Not Used
9	Not Used	Not Used
10	Dark Green	Jumper (7)
Quarter Bridge (NI-9945)		
Terminal Number	**Wire Lead**	**Wire Designator**
0	Red	Positive
1	White	Negative
2	Black	Ground

2. LabView Data Acquisition Procedure

The experimental data was collected via National Instrument's LabView Signal Express software suite, edition 2012. The LabView data acquisition software was configured to accept four modules for a total of 16 inputs. As shown in Table 7, the sample size was set to continuous to capture the entire strain and force fields. The rate was set to 30,000 Hz for the structure design analysis and 3,000 Hz for the composite sheet tension tests. All other data remained the same for the structure and tension analysis.

Table 7. LabView Signal Express Inputs. Source: [2].

Strain Setup	Signal Input Range Max	1 m
	Signal Input Range Min	-1 m
	Scaled Units	Strain
	Gage Factor	2.15
	Gage Resistance	350 ohm
	Vex Source	Internal
	Vex Value (V)	2.5
	Strain Configuration	Quarter Bridge I
	Lead Resistance	0
Force (Bridge) Setup	Signal Input Range Max	500
	Signal Input Range Min	0
	Scaled Units	Pounds
	Bridge Type	Full Bridge
	Vex Source	Internal
	Vex Value (V)	2.5
	Bridge Resistance	350 ohm
Timing Settings	Acquisition Mode	Continuous Samples
	Samples to Read	1500
	Rate (Hz)	30000

LIST OF REFERENCES

[1] Y. W. Kwon, "Study of fluid effects on dynamics of composite structures," *ASME Journal of Pressure Vessel Technology*, vol. 133, pp. 031301–6, Jun. 2011.

[2] T. South, "Fluid-structure interaction in a fluid-filled composite structure subjected to low-velocity impact," M.S. thesis, Department of Mechanical and Aerospace Engineering, Naval Postgraduate School, Monterey, CA, USA, 2016.

[3] Z. Aslan, R. Karakuzu, and B. Okutan, "The response of laminated composite plates under low-velocity impact loading," *Composite Structures*, vol. 53, pp. 119–127, Oct. 2002.

[4] R. Connor, "Fluid-structure interaction effects on composites under low-velocity impact," M.S. thesis, Department of Mechanical and Aerospace Engineering, Naval Postgraduate School, Monterey, CA, USA, 2012.

[5] M. Violette, "Fluid-structure interaction effect on sandwich composites," M.S. thesis, Department of Mechanical and Aerospace Engineering, Naval Postgraduate School, Monterey, CA, USA, 2011.

[6] R. McCrillis, "Dynamic failure of sandwich beams with fluid-structure interaction under impact loadings," M.S. thesis, Department of Mechanical and Aerospace Engineering, Naval Postgraduate School, Monterey, CA, USA, 2010.

[7] D. Varas, R. Zaera, and J. Lopez-Puente, "Experimental study of CFRP fluid-filled tubes subjected to high-velocity impact," *Composite Structures*, vol. 93, pp. 2598–2609, May 2011.

[8] J. A. Artero-Guerrero, J. Pernas-Sanchez, J. Lopez-Puente, D. Varas, "Numerical analysis of CFRP fluid-filled tubes subjected to high-velocity impact," *Composite Structures*, vol. 96, pp. 286–297, Oct. 2012.

[9] J. A. Artero-Guerrero, J. Pernas-Sanchez, J. Lopez-Puente, and D. Varas, "On the influence of filling level in CFRP aircraft fuel tank subjected to high velocity impacts," *Composite Structures*, vol. 107, pp. 570–577, Sep. 2014.

[10] Y. W. Kwon and J. D. Bowling, "Dynamic responses of composite structures coupled through fluid medium," *Multiscale and Multidisciplinary Modeling, Experiments and Design*, vol. 1, March 2018.

[11] "Economy plate carbon fiber sheets." Dragon Plate. Accessed January 5, 2018. [Online]. Available: http://dragonplate.com/ecart/categories.asp?cID=91

[12] R. D. Firouz-Abadi, H. Haddadpour, and M.A. Kouchakzadeh, “Free vibrations of composite tanks partially filled with fluid,” *Thin-Walled Structures*, vol.47, pp. 1567–1574, Jul. 2009.

[13] S. Rebouillat and D. Liksonov, “Fluid-structure interaction in partially filled liquid containers: A comparative review of numerical approaches,” *Computers and Fluids*, vol. 39, pp. 739–746, Jan. 2010.

[14] Y. G. Chen, K. Djidjeli, and W.G. Price, “Numerical simulation of liquid sloshing phenomena in partially filled containers,” *Computers and Fluids*, vol 38, pp. 830–842, Sep. 2008.

[15] H. Akyildiz and N. E. Unal, “Sloshing in a three-dimensional rectangular tank: Numerical simulation and experimental validation,” *Ocean Engineering*, vol. 33, pp. 2135–2149, Mar. 2006.

[16] M. Pentaleri, “Bifurcation Test Results,” internship work, Department of Mechanical and Aerospace Engineering, Naval Postgraduate School, Monterey, CA, USA, 2016.

INITIAL DISTRIBUTION LIST

1. Defense Technical Information Center
   Ft. Belvoir, Virginia

2. Dudley Knox Library
   Naval Postgraduate School
   Monterey, California